https://ntrs.nasa.gov/search.jsp?R=19710024608 2018-07-24T12:02:58+00:00Z

N71-34084

THEORETICAL CHEMISTRY INSTITUTE

THE UNIVERSITY OF WISCONSIN

LASER INDUCED GAS BREAKDOWN: SPECTROSCOPIC AND CHEMICAL STUDIES

Philippe de Montgolfier

CASE FILE COPY

WIS-TCI-442X

21 June 1971

MADISON, WISCONSIN

ERRATUM TO WIS-TCI-442X

Page 14, line 9 should read :

beams technique should be very interesting. Nevertheless N. K. Berezhetskaya (18) et al. report that in H_2 at pressure as low as 10^{-4} to 10^{-5} torrs the leading process was the ionization of the molecule leading to the formation of the H_2^+ ion and not the dissociation process. Above the breakdown's threshold, the energy between .....

Page 16, add reference 18 :

18. N. K. Berezhetskaya, G. S. Voronov, G. A. Delone, N. B. Delone and G. K. Piskova, Soviet Physics JETP 31, 3, 403 (1970).

LASER INDUCED GAS BREAKDOWN: SPECTROSCOPIC AND CHEMICAL STUDIES *

by

Philippe de Montgolfier

ABSTRACT

In this paper we report the results of several investigations on laser induced gas breakdown. These experiments included, time resolved spectroscopy, direct detection of H atoms, chemical reactions; each of them provided insight into the behavior of the medium at different times. Comparison of the intensity of the observed signals showed that the species formed were probably created during collisions with electrons. In addition, no primary multiphotonic absorption and no macroscopic chemical reaction were observed below the breakdown threshold.

- -

* This research received financial support from: commissariat a l'Energie Atomique, Centre National de la Recherche Scientifique, and from the National Aeronautics and Space Administration Grant NGL 50-002-001.

I. INTRODUCTION

By focusing a Q switched laser beam, one can get an intense energy flux density ($\sim 10^{15}$ w/cm^2). Above a threshold density there is a breakdown of air at the focus of the lenses:[1-5] an intense blue-white ball appears accompanied by a clapping and a sharp reduction of the laser beam transmitted through the focal zone. There is also a pressure threshold, a function of the gas, under which nothing happens. The elementary processes are very complex and numerous:

1) creation of the first electrons

2) heating of these electrons by inverse Bremsstrahlung electron-neutral, or electron-ion

3) emission of light by Bremsstrahlung

4) diffusion out of the focal zone

5) ionizing collisions

6) recombinations of ions and electrons

7) elastic and inelastic electrons

8) expansion of the plasma and shock waves: macroscopic movements of the plasma.

In order to analyze such a complex and rapidly evolving system, many different methods have been used. It is not our purpose to review here all the results obtained. We will recall only that, after an initial period of time, there is a multiplication of electrons, in a very fast cascade, by mainly the mechanisms 2 and 5 above. Inverse Bremsstrahlung is much more efficient in electron-ion collisions than in electron-neutral one. Therefore, when the number of ions is sufficient there is a tremen-

dous heating of the plasma, expansion, and often shock waves. After the extinction of the laser beam, the plasma cannot increase its energy, and there is a dissipation of energy. By lowering the gas pressure, one can control the development of the cascade and hopefully study the primary processes creating the first electrons.

The different theories proposed in order to explain the primary processes of laser induced gas breakdown[1] do not require that every atom or molecule excited to a discrete electronic level must be ionized later. In numerous studies, attempts have been made to measure at different pressures the number of electrons or ions created,[2-4] and the light emitted by the plasma.[5] Recently, chemical reactions have been initiated by laser induced gas breakdown.[6-9] But unfortunately experiemntal conditions varied in all these experiments and it is difficult to compare the results.

In the following report we describe experiments, partially published elsewhere,[10-12] in which are compared the evolutions of different particles relevant in the medium's dynamics, including electrons, excited states, atoms and products of reactions. By spectroscopy one can make conspicuous the radiation of bremsstrahlung of electrons and the radiative desexcitation of particular excited states. The hydrogen atoms created by interaction of the laser beam and a flow of molecular hydrogen are detectable with a semiconductor probe. Finally some chemical reactions may be initiated.

Thus one can follow the evolution of the irradiated medium through time and know the origin of the excited species. The two last types of

experiments can also be considered as means of detection giving an upper bound to the number of molecules dissociated by multiphotonic absorption.

II. SPECTROSCOPIC STUDY

A. Experimental Apparatus

We used a LASER CILAS VD 160 having the following characteristics: output energy = 3J, λ = 1.06μ, FWHM time = 30 ns, divergence of the beam = 5×10^{-4} rd. The electrical and optical setup (Fig. 1) is fully described elsewhere.[13-14] A double monochromator HUET M225 using two optical gratings with 610 lines per millimeter, blazed for 5000Å, was coupled with a photomultiplier tube 56CVP or 53AVP(FWHM of output pulse = 5 ns). The output pulses were monitored by an oscilloscope CRC 100 MHZ which was triggered by a photocell CSF F9096. The photomultiplier was triggered via a coaxial line (50 Ω) to give the proper time delay. The spectral resolution was 5 Angström and under our best conditions it was not possible to detect less than 10^3 photons per second at the focal point (f = 8 cm) of the laser beam.

B. Results

The spectral lines NII (4627Å, 5007Å) in nitrogen, HeI (5876Å) and HeII (5686Å) in helium, H_α(6563Å) in molecular hydrogen were studied in particular. In each case we observed an oscillogram showing three peaks corresponding to three luminous impulses appearing one after the other. In Figure 2 the results of H_α line are reported.

The first peak appeared before the maximum impulse of the laser beam and earlier and earlier as the gas pressure was increased. It did not vary much with the wave length observed and was due to the bremsstrahlung radiation of the electrons. In Figure 3 the intensity of this peak is plotted against the gas pressure.

We have seen elsewhere[10,13] that these results can be predicted by a model which ignores all inhomogeneities in the focal volume. Further simplifications give some insight on the differences of behavior of gases without any calculation: the evolution equation for the number of electrons has one term taking account of the rate of ionization (rate of energy increase by inverse bremsstrahlung divided by a threshold energy $\simeq$ ionization potential) and one other taking account of the losses by diffusion out of the focal volume. The diffusion constant is inversely proportional to the mass of the molecule, and therefore the losses are more important for helium than for argon or oxygen. Inverse bremsstrahlung cross sections increase with the energy of electrons much faster for heavy gases than for light ones, and as the ionization potential of helium is the highest, the rate of production of electrons by ionizing collisions will be low when compared to other gases, and less sensitive to gas pressure.

A second peak, which appeared after the extinction of the laser beam, was centered on the spectral lines of the gas. Its decay time varied with the gas between several hundred and several thousand nanoseconds. By examining different points of the focal zone, we saw that the plasma was not homogenous and had two centers which were more intense. Nevertheless the decay time of the signal was the same at any part within the plasma,

and one can assume that the processes giving rise to the excited states were identical throughout the plasma. We were able to compute the variations with time of the electronic density N_e and T_e of the plasma by studying the line's shapes and their stark broadening: in Figure 4 we present the results for H_α line. One can see that T_e is stabilized for several microseconds while N_e is still decreasing. These results agree with those recently reported for Helium.[5]

In the triparticular process,

$$H^+ + 2e \rightarrow H + e^*$$

electrons increase their kinetic energy, and this gain can compensate for the losses in inelastic collisions for a time. During this period of time, collision cross sections were constant, and the decay of the second peak paralleled very closely the variation of N_e. Therefore the corresponding excited states were probably produced in processes of first order with respect to electrons, such as:

$$H + e(\varepsilon_1) \rightarrow H^* + e(\varepsilon_2) \quad .$$

Numerous species and processes play a role in plasma's dynamics. In order to calculate T_e and N_e we supposed that the hypothesis of local thermodynamic equilibrium (LTE) applied. It could not be so if the process described above was predominant in the plasma's behavior. Actually we think that it plays a very small role and that evidence of the main processes could be investigated in the ultraviolet region.

The area under the second peak is plotted in Figure 5 versus the gas pressure for the H_α and NII 4627Å lines. At low pressures we could

not see any inflection of the curves corresponding to the excited states created by multiphotonic absorption. In particular, for helium, the light emitted in the transition 3d $^3D \rightarrow$ 2p ^3P_o, which is especially intense at ordinary pressure, did not show any irregularity at low pressures. This will be discussed in Part V.

The third peak has been studied recently.[16,17] It was centered on spectroscopic lines and appeared 300 ns or several μs after the second signal, according the part of the focal region examined: this result may be explained by assuming that the liminous zone was displaced toward the laser with a speed of 10^4 or 10^5 cm/s. Its decay time is analogous to the decay time of the second peak, and the limit pressure of appearance is larger.

C. Sensibility of Detection and Breakdown's Threshold

The overall characteristics of the detection are:

solid angle studied: 10^{-2} steradians

quantal efficiency of the photo cathode: 10%

maximal gain: 10^6

time constant of the R c circuit of charge: 0.7 ns

In the most unfavorable case, i.e. if a completely uniform distribution of excited states is created by direct multiphotonic absorption during the laser pulse, we would have been able to detect 10^5 desexcitations if the lifetime of excited states did not exceed 50 nanoseconds.

Because of the very rapid increase with pressure in the intensity of the radiation emitted from the gas at fixed laser energy, we can define a threshold pressure of breakdown. This concept is very useful for com-

paring different gases but has no precise definition . As we define the threshold, it corresponds to the pressure at which the electronic cascade develops very rapidly. At constant pressure we can also define a power threshold.

III. DIRECT DETECTION OF HYDROGEN ATOMS

A. Experimental Apparatus

The laser beam was focused in a glass balloon.[11] The focus of the lens (f = 8 cm) was on the axis of a glass tube (diameter = 2 mm) which served to introduce a large flow of H_2 . A TiO_2 probe, whose distance to the focus can be varied and measured, was set on the same axis (figure 6). The laser beam was directed perpendicular to this axis. The chemisorption of H atoms on TiO_2 has been extensively studied elsewhere:[11,12] the change in conductivity of the probe, due to the absorption is proportional to the local atomic concentration. One can show that H atoms created in the ionized volume and its vicinity were transported to the detector by the gaseous flow.[11,13]

B. Results

Measuring the atomic concentration at different distances from the focus is equivalent to studying the homogeneous recombination of radicals at different times. Taking the usual value of the speed constant of this three particle process $2\ 10^{-32}\ (cm^3)^2\ s^{-1}$ the recombination law is:

$$\frac{1}{[H]} - \frac{1}{[H_o]} = 6\ 10^{-3} t \quad .$$

A small part of the energy of the laser beam is absorbed by the plasma and later thermalized. This changes the constant of recombination negligibly, and we may neglect the effect of this absorption of energy from the laser.

The experimental law is:

$$\frac{1}{[H]} - 1.75\ 10^{-3}\ x = 0.5t\ x$$

where x is a constant which is a characteristic of the detector and whose value is unknown. But the comparison of these two expressions allows one to determine x, and therefore give an absolute measure of the local concentration of H atoms at different times.

In Figure 7 and 8 we have plotted the atomic concentration in the focal volume, just after the extinction of the plasma, as a function of the energy of the laser beam at 760 torr and of the gas pressure at constant energy.

Below the breakdown's threshold we were not able to detect any H atoms. Under such conditions, taking account of the small focal volume (there is no plasma expansion), it would have been necessary to have 10^{11} dissociated molecules in order to detect any atoms.

IV. CHEMICAL REACTIONS

Pyrex glass cells, of spherical or cylindrical shape, contained between 5 and 100 cm^3 of the gas to be irradiated. The main product of reaction was analyzed by gas phase chromatography or mass spectroscopy. We studied[11] the photolysis of acetaldehyde, the isotopic exchange

between H_2 and D_2, and some explosive mixtures: hydrogen and oxygen, hydrogen and chloride, acetone and oxygen, acetaldehyde and oxygen, propane and oxygen. Before the laser beam exposure, all the binary mixtures were equimolar.

Looking at the light emitted by the focal volume allowed us to determine the approximate development of the plasma at the time of the extinction of the laser beam.

We studied at first the reaction $H_2 + D_2 = 2HD$ by measuring the final concentration of HD. In Figure 9 this quantity is plotted at 760 torr and 300°K against the laser beam energy. Below the threshold energy of 0.8J we did not observe any HD. Analogous results were obtained for all other reactions.

Under the standard conditions of temperature and pressure the reaction $H_2 + C\ell_2 = HC\ell$ can be initiated photochemically and is explosive. Porter[7] observed this reaction below the breakdown threshold and interpreted it by assuming a dissociation of chloride by simultaneous absorption of two photons (ruby laser). With our laser (Neodinium), one needs a three photon absorption to get the same result, and this mechanism is less probable. Nevertheless, if we compare this number to the ten photons necessary for the multiphotonic ionization of chloride, one could expect to see a photodissociation in spite of the selection rules.

The speed of branching of the reaction $2H_2 + O_2 = 2H_2O$ is small at standard T and P when compared to the speeds of recombination of the radicals involved. Therefore one cannot initiate an explosion by creating locally a high atomic concentration. However an explosion occurred each

time the mixture was irradiated with a laser beam where energy was greater than the threshold: this is strong evidence for the important role played in the evolution of the reaction by the transformation of a part of the photonic energy of the laser beam into thermal energy of the gas.

When there is no breakdown, this energy transfer is negligible and we studied theoretically at 300°K and 600°K the progress of the reaction $H_2 + D_2 = 2HD$: the free radicals diffused from the center of the reactor and reacted together at the same time. Under our experimental conditions at least 10^{11} or 10^{15} molecules had to be dissociated in order to induce a detectable reaction. Optimizing all the physical parameters would lower this number to 10^{12}.

V. DISCUSSION

All the experiments reported here might have given more precise results. This would have required very sophisticated apparatus and would have precluded the possibility of investigating more than a single aspect of the gas's evolution.

Our results can be analyzed from several different points of view: chronometry, origin of the involved particles, multiphotonic absorption, chemical reactions.

The spectroscopic study allowed us to isolate three effects contributing to the emission of light from the plasma. The bremsstrahlung radiation from the electrons appeared first, reached its maximum at the extinction of the laser beam, and then decreased very rapidly. The radiative de-excitation of atoms became very important several hundred nanoseconds later. It is well known that during this interval the plasma

expands greatly. The third peak might correspond to an emission of light occurring in a supersonic blast in the direction of the laser: this is the simplest interpretation of our results, but of course more detailed experiments are needed. In the case of molecular hydrogen, we determined the number of atoms present in the ionized volume after complete extinction of the plasma, i.e., after a fraction of a millisecond. We followed the homogeneous recombination of these atoms and also the H_2 and D_2 exchange reactions. During these different moments of the evolution of the media, we had many evidences for macroscopic movements of the media (cf Appendix 2).

The spectroscopic study allowed us to isolate three effects contributing to the emission of light from the plasma. The bremsstrahlung radiation from the electrons appeared first, reached its maximum at the extinction of the laser beam, and then decreased very rapidly. The radiative de-excitation of atoms became very important several hundred nanoseconds later. It is well known that during this interval the plasma expands greatly. The third peak might correspond to an emission of light occurring in a supersonic blast on the direction of the laser: this is the simplest interpretation of our results, but of course more detailed experiments are needed. In the case of molecular hydrogen, we determined the number of atoms present in the ionized volume after complete extinction of the plasma, i.e. after a fraction of a millisecond. We followed the homogeneous recombination of these atoms and also the H_2 and D_2 exchange reactions. During the time of evolution of the medium we observed some macroscopic movements of the plasma (cf. appendix 2).

The bremsstrahlung effect is the emission of light occurring when electrons interact with ions or neutral particles. As a first approximation, ignoring the energy distribution of electrons, one can consider that the maximum intensity of this first peak is a measure of the square of the number of electrons in the plasma at the time of extinction of the laser beam. We have shown that the decrease in intensity of the spectral line H_α is of the first order with respect to the number of electrons, and concluded that the excited states involved were probably created by inelastic collisions between electrons and neutrals. On Figure 10 we have plotted the square root of the bremsstrahlung intensity, the H_α line intensity, and the number of atoms extrapolated from the measurements made with the TiO_2 detector, versus the gas pressure. One can see that it is impossible to distinguish the three curves. This result supports the interpretation given above for the origin of the excited states, and also that the atoms are probably created by collisions of molecules with electrons, and not by such processes as, for example:

$$e + A_2^+ \rightarrow 2A$$

This concerns only hydrogen. The line NII 4627Å cannot be interpreted in the same way because its intensity varies more than the bremsstrahlung intensity with nitrogen pressure: actually it is not surprising because it corresponds to an emission from an ionic excited state and is proportional to a power of the electronic denisty greater than two.

One can consider also that the excellent superposition of the three curves of Figure 10 demonstrates that the inhomogeneities and macroscopic movements are not important for the understanding of the light emission and of chemical reactions, in the domain of pressure studied.

The light emission by bremsstrahlung was a quasi continuum. Therefore at low pressures low spectral solution would give the strongest signal. Under such conditions P. Agostini et al. have seen the beginning of the electronic cascade. It is obviously impossible to get the benefit of such conditions in the detection of spectral lines and we did not see any primary processes. As excitations of atoms and dissociations of molecules need many fewer photons than ionization one would expect these processes to be more probable. The results of our experiments showed that there were less than 10^{11} molecules of hydrogen dissociated by multiphotonic absorption just below the breakdown's threshold. It is more difficult to give a bound for the number of excited atoms because we studied only a few lines and because the efficiencies of the different processes of atomic de-excitation are not known. There were less than 10^5 photons emitted in each spectral line. A study of the ultraviolet region would give some information on the lower excited states but will encounter the same difficulty.

It seems impossible to initiate chemical reactions and explosions in the high pressure domain if there is no plasma. Under the best conditions 10^{12} molecules would have to be dissociated at the focus of the lens in order to observe an isotopic exchange between H_2 and D_2 at a macroscopic scale. But we have shown by direct detection that there

are less than 10^{11} atoms and spectroscopic studies suggested this number is several order of magnitude smaller.

We have shown in Appendix 3 that, in the domain of pressure studied here, it is likely that the multiphotonic absorption involves impurities or collision-induced absorption: in such a case it should be normal to have not seen any excited state or atoms below the breakdown threshold. But at pressure lower than 1 torr, multiphotonic absorption involves for sure the gas molecules, and therefore, one can perhaps see it: molecular beams technique should be very interesting. Above the breakdown's threshold, the energy transfer between the laser beam and the gas plays an important role in the kinetics of the reaction. Unlike with many other techniques, it is possible by focusing a laser beam to achieve a spherical symmetry very interesting in the investigation of homogeneous reactions. Furthermore, the laser induced gas breakdown can be very useful for studying the dynamics of explosions.

ACKNOWLEDGEMENTS

The experimental part of this work has been performed at the "Centre de Cinetique Physique et Chimique" du CNRS-Nancy-France, with the participation of P. Dumont and Y. Mille. We would like to thank Professor P. Le Goff and J. Villermaux for their enthusiastic support, and Dr. C. Rosenthal for discussions on the cascade.

REFERENCES

1. See for example, L. V. Keldysh, Soviet Physics JETP, 20, 1307 (1965); H. B. Bebb and A. Gold, Phys. Rev. 143, 1 (1966); Y. Gontier, M. Trahin, Phys. Rev. 172, 83 (1968); Y. Mille, Thesis, Nancy France 1971.
2. R. G. Meyerand, A. F. Haught, Phys. Rev. Letters 11, 401 (1963).
3. R. W. Minck, J. Appl. Physics 35, 252 (1964).
4. P. Agostini, J. P. Bonnal, G. Mainfray, C. Manus, C. R. Acad. Sci. Paris 266, 1034 (1968).
5. See for example, W. F. Braerman, L. R. Stumpfel, H. J. Kunze, J. Appl. Physics 40, 2549 (1969).
6. J. F. Verdieck, Nucl. Appl. 6, 474 (1969).
7. G. Porter, Nature 215, 502 (1967).
8. L. M. Epstein, K. H. Sun, Nature 211, 1173 (1968).
9. J. H. Lee, R. Knystautas, A. IAA Journal 7, 312 (1968).
10. P. Dumont, Y. Mille, Ph. de Montgolfier, C. R. 1971.
11. P. Dumont, Ph. de Montgolfier, P. Le Goff, J. de Chim. Phys., 1971.
12. P. Dumont, Ph. de Montgolfier, J. de Chim. Phys., 1971.
13. P. Dumont, Thesis, Nancy 1970.
14. Y. Mille, diplome de etude approfondies, Nancy 1968.
15. Y. Zel'dovich, Yu P. Raizer, Soviet Physics JETP 20, 772 (1965).
16. V. Chalmeton, R. Rapoular, C. R. Acad. Sci. Paris 264, 213 (1967).
17. G. Lampis, S. C. Brown, Physics Fluids 11, 1137 (1968).

APPENDIX I

Notation:

ε	energy of one electron
I	ionization potential of a molecule
$n(\varepsilon, t)$	density of electrons with energy in the interval $[\varepsilon, \varepsilon + d\varepsilon]$ at time t
N(t)	total density of electrons at time t
$a(\varepsilon)$	absorption coefficient by inverse bremsstrahlung electron-neutral corrected for the stimulated emission
ν	laser frequency
σ	momentum transfer cross section
G(t)	quantum flux density of the laser beam at time t
f	focal length of the focusing lens
α	divergence of the laser beam
σ_i	ionization cross section
T(t)	electronic temperature of the plasma at time t

Here we are interested in the general development of the electron cascade, and in particular, in the period of electron multiplication which follows the appearance of the first multiphotonic electrons. Many theoretical studies have already been made[1-6], but it appears that the first calculations were not very refined and that the latter two[5-6] did not take into account the electron energy distribution. We will

develop general expressions which give rise naturally to different approximations.

1. General Theory

The time evolution of the electron density, with energy in the interval [ε , $\varepsilon + d\varepsilon$] is described by the transfer equation:

$$(1) \quad \frac{\partial}{\partial t} n(\varepsilon, t, r) = \nabla^2 (D n) + \text{Inverse bremsstrahlung, ionisation, elastic collisions, electron attachment, recombination electron-ion processes} + \ldots$$

Numerical integration of this equation is difficult because the elementary processes are very fast during the cascade and therefore the integration steps are necessarily very small. However, if we know the electron energy distribution, then it is possible to make a transformation which reduces (1) to a set of coupled differential equations which are simpler to solve.

When the electron energy distribution is known, integration of (1) with respect to the energy gives the electron balance equation. Inverse Bremsstrahlung and elastic collision processes which lead to energy transfers but do not alter the number of electrons, play no role in this equation.

$$(2) \quad \frac{\partial}{\partial t} N(t, r) = \int_0^\infty [\text{equation } 1] \, d\varepsilon$$

In a similar way the energy balance equation may be obtained by taking the first moment of (1) with respect to the total energy. Thus:

$$\int_0^\infty (I + \varepsilon) \frac{\partial}{\partial t} n(\varepsilon, t, r) \, d\varepsilon = \int_0^\infty (I + \varepsilon) \times (\text{equation } 1) \, d\varepsilon$$

where the ionization contributions vanish because the total energy is conserved in such a process, and the elastic collision contribution is negligible since the electron mass is small compared to the molecular and ionic masses. If the energy distribution is characterized by several parameters the one may use the corresponding moments of (1) to obtain their variation with time.

An examination of the cross sections for the various elementary processes shows that the electron energy will not increase significantly above the ionization potential of the neutrals. One may therefore suppose that in any ionizing collision the resulting electrons will possess low energies. Hence, using Equation (1) it is possible to calculate, as a function of time, both the energy of an electron which was produced at time $t = 0$ with a low kinetic energy, and the probability of its disappearance. Thus, using the second postulate of statistical mechanics, one can derive the energy distribution of the ensemble at a given instant.

For completeness, it is necessary to consider the transfer equation governing the radiation density of the laser beam. However, the flux density of photons is essentially constant throughout the focal volume up until the period of intense heating, which follows the period described above, and so one may ignore this equation.

2. Study of the Elementary Processes From a Boltzmann Distribution

Since binary elastic collisions are far more frequent than the tertiary collisions, electron-atom-photon, we will use the quasistationary

state approximation: the fast electron collisions produce an energy distribution as a function of time which is independent of the other processes. For the simplicity we will approximate the true distribution by a Maxwellian distribution:

$$(3) \quad n(\varepsilon, r, t) = \frac{2\pi N(r,t)\sqrt{\varepsilon}}{(\pi kT)^{3/2}} e^{-\frac{\varepsilon}{kT}}$$

We will now consider the various processes involved in (2) and (3):

Inverse bremsstrahlung electron-neutral: Zeldodvich (1) has shown that when, $h\nu \ll \varepsilon$, the absorption coefficients for the inverse bremsstrahlung and the stimulated emission of one electron in the field of a neutral reduce to the term describing the heating of an electron gas irradiated by an HF field:

$$a(\varepsilon) = \frac{4\pi e^2 \sigma \nu}{mc(2\pi\nu)^2}$$

Here σ is the momentum transfer cross section which is assumed to be independent of the electron energy, although in Fig. 11 we report the true dependence of σ on the energy. In this process the energy absorbed by the electron gas per unit time and volume is:

$$a(\varepsilon)\, h\nu\, n(\varepsilon)\,(P-N)\, G$$

and an integration over the energy range of the electrons we obtain

$$(4) \quad \frac{2\sqrt{2}\, e^2 \sigma h G (P-N) N \sqrt{kT}}{(\pi m)^{3/2} c\nu} = A\,(P-N)\, N \sqrt{T}$$

In the transfer equation (1) the inverse Bremsstrahlung term is

$$G(P-N)\left[a(\varepsilon-h\nu)\, n(\varepsilon-h\nu) - a(\varepsilon)\, n(\varepsilon)\right] \approx G(P-N)\, h\nu \frac{\partial}{\partial\varepsilon}(an)$$

and it is easily seen that the zero and first moments of this equation with respect to the energy yield zero and equation (4) respectively.

Inverse bremsstrahlung electron-ion: the absorption coefficient $b(T)$ of a photon by an electron in the presence of $N(t,r)$ ions is, following Pitzer (7):

$$(5) \quad b(T) = \frac{4}{3}\left(\frac{2\pi}{3kT}\right)^{1/2} \frac{e^6}{c\, m^{3/2} \nu^2} N^2(t,r) = \frac{J N^2}{T^{1/2}}$$

In order to take into account the stimulated emissions one has to multiply $b(T)$ by $\left(1 - e^{-\frac{h\nu}{kT}}\right)$.

Ionization: We have already reported that the electron energy is never much greater than the ionization potential of the neutrals before the period of intense heating of the plasma: we will therefore assume that the ionization cross section σ_i is a linear function of energy:

$$\sigma_i = \sigma_0(\varepsilon - I)$$

Using this in conjunction with the expression $\langle \sigma_i \sqrt{\frac{2\varepsilon}{m}}\, n(\varepsilon) \rangle (P-N)$ for the rate of conversion of the neutrals we obtain:

$$(6) \quad \frac{2\sqrt{2kT}}{\sqrt{\pi m}} \sigma_0 \left[I + 2kT\right] e^{-\frac{I}{kT}} N(P-N)$$

$$= H\left[I + 2kT\right] e^{-\frac{I}{kT}} N(P-N)\sqrt{T}$$

In the derivation of this expression we have made no assumption on the partioning of energy between the two electrons after the collision.

Diffusion: The focal volume has cylindrical symmetry and therefore:

$$D \nabla^2 n = D \frac{\partial^2 n}{\partial r^2} + \frac{D}{r} \frac{\partial n}{\partial r}$$

In a complete treatment one should also take into account the energy dependence of the momentum transfer cross-section. For numerical application we will take into account the fact that diffusion is unimportant for pressures greater than 100 torrs as was shown by C. G. Morgan (5). The focal volume is a cylinder of radius $f\alpha$ and length L . We will suppose that the electron concentration is homogeneous throughout this volume and vanishes outside. In neglecting the losses at the ends of the cylinder one finds that:

$$\left(\frac{\partial n}{\partial t}\right)_{diffusion} = \frac{\pi}{6 P f^2 \alpha^2} \sqrt{\frac{2\varepsilon}{m}}\, n$$

which becomes after integration:

$$\left(\frac{\partial N}{\partial t}\right)_{diffusion} = \frac{\pi^{3/2} \sqrt{2kT}}{3 \sigma f^2 \alpha^2 \sqrt{m}} \frac{N}{P} = DD \frac{N}{P} \sqrt{T}$$

Electron attachment and recombination electron ion: This names cover processes which are quite different and often not very well known. It would not be very difficult to take it into account, but our aim, here, is not to perform the best calculation that one can make. A good study of the importance of the recombination processes had been made by Morgan (5). Electron attachment processes are important for O_2 but not for rare gases.

3. Results and Discussion

The transfer equation reduces to the two equations:

$$(7) \quad \frac{\partial N}{\partial t} = D \frac{\partial^2 N}{\partial r^2} + \frac{D}{r} \frac{\partial N}{\partial r} + H(I + 2kT)\, e^{-\frac{I}{kT}}\, N(P - N)\sqrt{T}$$

$$(8) \quad \frac{3}{2} k \frac{dT}{dt} = A(P - N)\sqrt{T} + \frac{JN}{\sqrt{T}} - H\left[I + \frac{3}{2}kT\right]\left[I + 2kT\right]\sqrt{T}\, e^{-\frac{I}{kT}}(P - N)$$

if we neglect electron attachment and recombination.

Thermal equilibrium: at the beginning of the cascade and the inverse bremsstrahlung electron-ion is negligible. Therefore:

$$(9) \quad \frac{3}{2} k \frac{dT}{dt} = \left[A\sqrt{T} - H\left(I + \frac{3}{2}kT\right)\left(I + 2kT\right)\sqrt{T}\, e^{-\frac{I}{kT}}\right] P$$

From this equation it follows that the temperature is a function of P.t and is independent of the number of primary electrons. After a while thermal equilibrium is attained. In Figure 12 we show the variation of this equilibrium temperature with the power of the laser beam obtained with model computations of argon and helium. It is remarkable that the temperature of the focal volume is independent of the diffusion processes in so far as the I. B. electron-ion is unim-

portant: in particular if the initial temperature and the laser intensity are uniform throughout the focal volume, then the temperature remains uniform.

When the electron density becomes significant prior to the extinction of the laser beam the term $\frac{JN}{\sqrt{T}}$ comes into play, causing an increase in the electronic temperature: the heating effect thus induced gives rise to the macroscopic movements studied in Appendix 2.

Conditions for increase in the number of electrons

The electronic temperature is a function of Pt, and G, T(Pt, G) and one can compute the maximum temperature $T_M(P,G)$ attained in the duration, T , of the laser pulse. Further, the total number of electrons increases only if dN/dt becomes positive, or equivalently, if the pressure P satisfies

$$P \geq P_{lim} = \left[\frac{D D e^{\frac{I}{kT}}}{(I + 2kT) H} \right]^{1/2}$$

Hence we have a second function T(P) . The intersection of the curves representing these two conditions determines a critical pressure $P_c(G)$ below which no cascade can occur. The breakdown threshold can be defined as the limiting pressure such that the I-B electron-ion process ceases to be negligible. Such a definition takes into account the phenomenon which causes the fast heating of the plasma.

The Monoenergetic Approximation: When the steady temperature is attained fast, one can neglect the transient state. In such a case, (8) gives dT/dt = 0 so that T = constant in equation (7), which

is equivalent to the equations used by other authors (5, 6). In this way we can know the mean energy of the electrons and do not need to guess it. With this proviso Morgan's analysis of the cascade is valid. However Mille[6] uses an equation for the elctron balance which involves an inverse Bremsstrahlung electron-neutral term, and the analyses made here suggest that it is incorrect.

If the electron-ion recombination and electron attachment processes are excluded, we have

$$(10) \quad \frac{dN}{dt} = \frac{A(P-N)N\sqrt{T}}{\left[I + \frac{3}{2}kT\right]} - DD\frac{N}{P}\sqrt{T}$$

This formula can be derived directly from physical intuition: one assumes that any electron possessing a greater total energy than $(I + \frac{3}{2}kT)$ will quickly ionize a molecule, and hence the rate of acquisition of this energy, $A(P-N)\sqrt{T}$, divided by this energy $(I + \frac{3}{2}kT)$, yields the average lifetime of one electron. The losses by diffusion are $DD\frac{N}{P}\sqrt{T}$, but again the derivation says nothing about the threshold temperature T.

<u>Numerical Results and Discussion</u>: Equations (7) and (9) we solved with:

$\alpha = 1.3 \; 10^{-3}$ radians

$f = 8$ cm

laser pulse : duration 40 ns and constant intensity P_M

$P \in [1,700]$ torrs

$P_M = 8.3 \; 10^{I}$ MW; $I = 1, 2, 3, 4$

$$1 \begin{cases} \sigma = 3 \; 10^{-16} \; cm^2 \\ \sigma_o = 5 \; 10^{-6} \; cm^2/ergs \\ I = 24, 46 \; eV \end{cases} \qquad 2 \begin{cases} \sigma = 1 \; 10^{-15} \; cm^2 \\ \sigma_o = 5 \; 10^{-6} \; cm^2/ergs \\ I = 15.68 \; eV \end{cases}$$

The model calculations 1 and 2 are for Helium and Argon respectively. In figure 13 we plot final density against the gas pressure. The experimental differences between Argon and Helium are well predicted. The time t_o taken for a stationary temperature to be attained is a decreasing function of the laser power.

Power of the laser beam (MW)

		8.3	83	830	8300
Helium	t_o s.	$8 \; 10^{-9}$	$7.6 \; 10^{-10}$	10^{-10}	$1.7 \; 10^{-11}$
Argon	t_o s.	$1.3 \; 10^{-9}$	$3.5 \; 10^{-10}$	$5 \; 10^{-11}$	$8.5 \; 10^{-12}$

It is seen that when the laser beam power is not too low the stationary state is reached very quickly and hence it would be a good approximation to take the temperature of the medium as a constant. However, we emphasize here that this temperature can be calculated from the energy equilibrium balance equation very simply, and there is no need to guess it.

In Figure 14a we have plotted T and N as a function of time for the model of argon at a pressure P = 70 Torr. Here we can see that the inverse Bremsstrahlung (electron-ion) process comes into play after 2.5×10^{-8} sec, when the electron density is of the order of 6.10^{16}/cc. When the gas is fully ionized the temperature increases

linearly with time. After 2.8×10^{-8} sec. the electronic temperature is already 10^{6}°K, and shock waves develop in the plasma as is shown in Appendix 2. Hence, the steady temperature is valid only at the beginning of the cascade.

Figure 14b the two curves $T = f(P)$ whose intersection determines the critical pressure for Helium. For argon one finds that critical pressures are very small.

No attempt has been made to optimize the parameters to obtain the best fit with experimental results. From Figure 11 we see that it is necessary to allow for the functional dependence $\sigma(\varepsilon)$, otherwise an optimisation will not be significant. Our purpose was to illustrate some general features of the cascade which are not often mentioned. An exact calculation would not be hard.

REFERENCES

1. Y. B. Zeldovich, Y. P. Raizer, Soviet Physics JETP 20, 772 (1965).
2. A. V. Phelps, Physics of Quantum Electronics, Puerto Rico 1965, Mc-Graw Hill, New York, 1966.
3. G. A. Askaryan, M. G. Rabinovich, Soviet Physics JETP 21, 190 (1965).
4. M. Young, Ph.D. dissertation, Univ. of Rochester (1967).
5. F. Morgan, L. R. Evans, C. G. Morgan, J. Phys. D, Appl. Phys. 4, 225 (1971).
6. Y. Mille, Thesis, Nancy, France 1971.
7. L. Spitzer, Jr., Physics of Fully Ionized Gases, Interscience (1956).
8. H. S. W. Massey, Electronic and Ionic Impact Phenomena 2, Oxford (1969).
9. J. B. Hasted, Physics of Atomic Collisions, Butterworth (1964).

APPENDIX II

Inhomogeneities and hydrodynamics of the plasma

The first studies of the laser induced gas breakdown by ultrafast photography showed two luminous zones growing very rapidly. The model we have presented in Appendix I takes no account of plasma inhomogeneities and macroscopic movements. However such phenomena were seen in our experiments.

When the monochromator is set at $\lambda = 10600\text{Å}$ the photomultiplier received only the light diffusing out of the plasma during its heating. The oscillogram (figure 15) showed two peaks, one arriving 10 ns after the other and their rleative intensity depending upon the focal region studied. A. J. Alcock (1) was unable to see the two peaks with a "slit-aperture" camera . The plasma seems to have two diffusing zones appearing one after the other. The velocity of propagation toward the laser is 10^7 cm/s.

We have plotted on Figure (16) the intensity of the H_α line, several hundreds of nanoseconds after the laser extinction, versus the focal region examined. Again one can see that there are two regions where the intensity is greater than at the focal center. This may be due not only to a nonhomogeneous electronic density, but also to nonhomogeneous electronic temperatures and to different H-excitation processes occuring in the two regions.

We did not calculate the electronic temperature at different locations within the focal volume, but as the decay time of the line H_α was

the same everywhere, we infer that there was in fact only one elementary process leading to the H_α excitation throughout the focal volume.

As mentioned earlier, the observations on the "third peak" suggested that, several microseconds after the laser extinction, a macroscopic displacement of the plasma takes place toward the laser.

Such inhomogeneities could not be entirely explained by imperfections of the focusing optics, since such an explanation would say nothing about the macroscopic movements observed at different times of the plasma development.

Ramsden and Savic (2), Champetier[3] invoke the creation of a pressure and temperature discontinuity near the focus of the lens to explain these macroscopic movements: an enhanced shock wave occuring in the region experiencing the laser beam would travel toward the focusing lens. Another explanation supports that the breakdown occurs when the electronic density is greater than a minimum value which is a function of the flux density; Raizer (4) shows that during the laser irradiation this minimum density occurs at points nearer and nearer the lens as time goes on. Veyrié (5) made the most extensive calculation and showed that for hydrogen, the enchanced shock wave is faster than Raizer's breakdown wave and is therefore the controlling factor in the vicinity of the breakdown conditions. He calculated a velocity of 0.8 10^7 cm/s, in excellent agreement with our experimental result and those of ultrafast photography.

On figure (17) we have pictured the two enhanced longitudinal waves and the two slower transverse waves. Under the critical conditions

surfaces 1 and 2 (figure 17) have the same velocity: the plasma absorbs and diffuses very little of the incident beam and therefore the heating is isotropic. At higher pressures 1) propagates faster because of the high electronic density and diffusivity whereas region 2) receives only a few photons. Daiber and Thompson (6), in a plasma of nitrogen under atmospheric pressure, have seen only a propagation toward the laser.

Our experimental results on the bremsstrahlung emission at different pressures and the model proposed for the development of the cascade allow us to understand the processes responsible for this different behavior. Furthermore it is evident that for helium the pressure domain, in which one could see a longitudinal propagation in both directions, would be larger than the corresponding domain for hydrogen. But for the heavy gases which showed a very sharp increase of the bremsstrahlung emission with pressure, we would not expect such a phenomenon except in the very vicinity of the threshold.

Plasma hydrodynamics have been studied by those interested in initiating thermonuclear reactions with a laser beam: the goal in these experiments was to confine the plasma and to get the highest temperature possible. But the chemical processes we are interested in begin only after the plasma extinction and therefore when the macroscopic movements are no longer important. Furthermore we have studied a small domain around the pressure threshold where the movements themselves are small. We think that our experiments support the assumption that under such conditions one can neglect the hydrodynamics of the plasma, and that the model used for the cascade is valid. The computation of the exchange

reaction, H_2/D_2, has not been made at the atmospheric pressure because at such high pressure the heat transferred from the laser beam to the gas may be important.

Therefore, depending on the aims of the experiments, one may work in the vicinity of the breakdown threshold and neglect the hydrodynamics, or above the threshold and take account of the macroscopic movements of of the plasma. Those interested in explosive reactions and propagation of deflagrations must obviously use high electronic and flux density in order to maximize the discontinuity at the focal center.

REFERENCES

1. V. V. Korobkin, A. J. Alcock, Phys. Rev. Letters 21, 1433, (1968).
2. S. A. Ramsden, P. Savic, Nature 203, 1217 (1964).
3. J. L. Champetier, C. R. Acad. Sci. Paris 261, 3954 (1965).
4. Y. Raizer, J.E.T.P. 21, 1009 (1965).
5. P. Veyrie, Joun. de Physique 31, 41 (1970).
6. J. W. Daiber, H. M. Thompson, Physics Fluids 10, 1162 (1962).

APPENDIX III

Origin of the First Electrons

Natural appearance of electrons in the focal volume is very unlikely. The probability of auto ionization of a hydrogen atom in an electric field of 10^7 V/cm is extremely low. Therefore different theories invoke a multiphotonic absorption of very high order in ($m\,h\,\nu \simeq I$ potential de-ionization), but they give cross sections of ionization which are too small. It is not surprising that perturbation theory leads to poor results because the "perturbation" by the electric field is of the order of magnitude of the unperturbed energy. Recently (1) a method of approximation based upon a unitary transformation, which suppresses the very intense electromagnetic field from the problem, has been proposed for bound states: the order of the multiphotonic process is less than would be predicted by previous theories.

In order to obtain experimentally the order in and the cross section a_m many authors have studied, at very low pressure (10^{-3} - 10^{-2} torrs), the number of electrons or ions created as a function of the power of the irradiating laser beam. A phenomenological equation of evolution of the electronic density is:

$$\frac{\partial n}{\partial t} = a_m N \left(\frac{P}{s}\right)^m + \text{terms studied in Appendix II}$$

The first term is the multiphotonic one of interest here. Taking account only of this term, V. Chalmeton derived the following expression for P_i ,

the threshold of appearance of electrons:

$$P_i = \pi f^2 \alpha^2 \left(2\pi^{3/2} L f^2 \alpha^2 a_m N \frac{b}{\sqrt{m}} \right)^{-\frac{1}{m}}$$

L = axial dimension of the focal volume

b = line constant of the laser impulsion.

$$N_t = \left(\frac{P_m}{P_i} \right)^m = \text{number of electrons}$$

Agostini[2] has interpreted some experiments on hydrogen under 10^{-3} torrs by a numtiphotonic absorption of order 9 for $\lambda = 1{,}06\mu$. But Blanc (3) reports that even at low temperature the initiating of a cascade can alter the multiphotonic order: therefore the number 9 is not necessarily exact, but must be close to the true one. A study of the dependence of P_i upon the gas pressure and the focal length of the lens has been made by Chalmeton (1 - 500 torrs)[4] It appears that the experiments are compatible with the predicted multiphotonic effect (4) only for gass pressures lower than 20 torrs. Above 30 torrs the results can be interpreted with an order equal to 2 . One can not avoid some impurities in the gas and if they have a very low ionization potential they may become important as the pressure increases. Aklaline impurities would need only 3 or 4 electrons to be ionized; taking account of the experimental and theoretical presumption (3,1) for an order smaller than that predicted by the relation $m h \nu \simeq I$, one cannot reject this explanation. One other explanation, proposed by Papoular, is the non resonant photoelectric effect: a multiphotonic absorption of very low order can occur during intermolecular collisions. Both explanations

suggest that the probability of excitation or dissociation of molecular hydrogen by multiphotonic absorption was very small in the domain of pressures studied in our experiments, and that the sensitivity of the detector does not account for the absence of such species. Under gas pressures lower than 1 torr the multiphotonic absorption takes place on the isolated moelcules, and our study should be done under such conditions.

But in a very recent paper Berezhetskaya et al. have studied the multiphotonic ionization of H_2 at very low pressure (10^{-5} - 10^{-4} torrs): H_2^+ ions are 100 times more numerous than H^+ ions, and they conclude that the process

$$H_2 + 15{,}4 \text{ eV} \rightarrow H_2^+ + e$$

is more probable than

$$H_2 + 4{,}5 \text{ eV} \rightarrow H + H$$

It is therefore not obvious that it will be possible to observe the dissociation of a molecule.

A very good survey of the current papers in this field has been made by Mille (6).

REFERENCES

1. H. R. Reiss, Phys. Rev. A 1, 803 (1970).
2. P. Agostini, J. P. Bonnal, G. Mainfray, C. Manus, C. R. Acad. Sci. Paris 266, 1034 (1968).
3. A. Blanc, Personal communication.

4. V. Chalmeton, Journal de Phys. 30, 687 (1969).

5. N. K. Berezhetskaya et al, Soviet Physics JETP 31, 3, 903 (1970).

6. Y. Mille, Thesis, Nancy, France (1971).

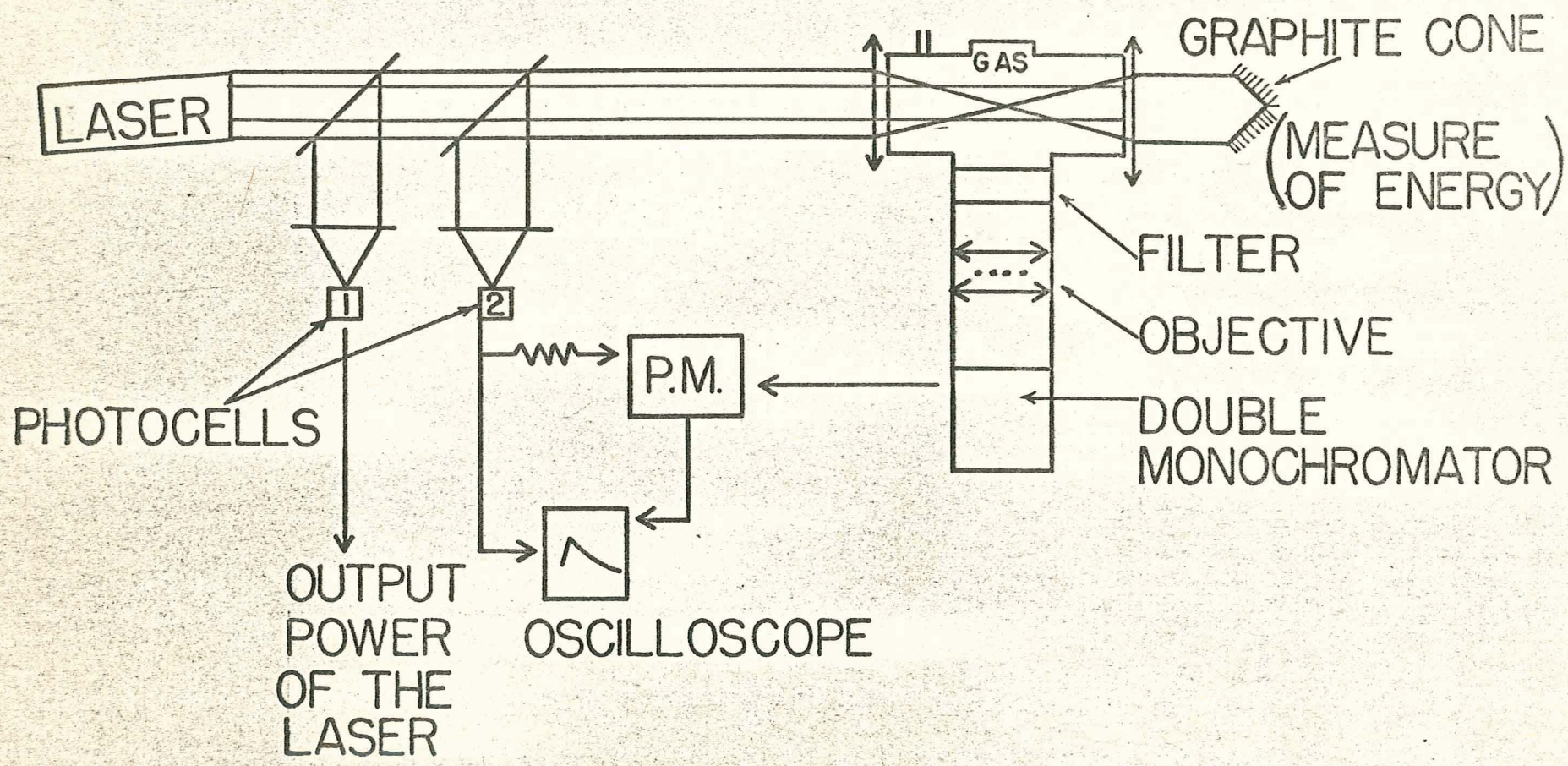

Figure 1: Block diagram of the apparatus

The photocell 2 triggers the oscilloscope and the photomultiplier P.M.

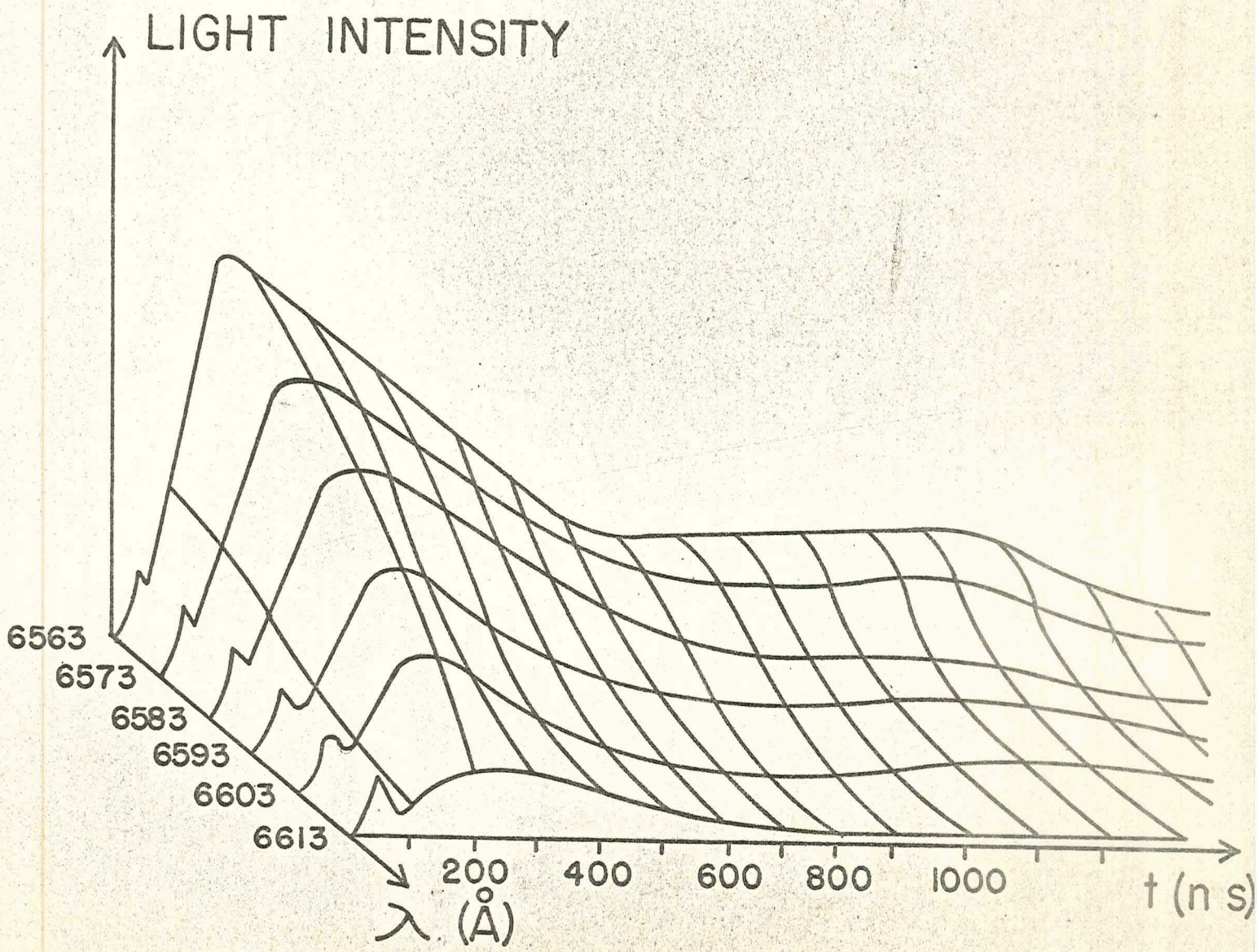

Figure 2: H_α line, light intensity = $f(t,\lambda)$

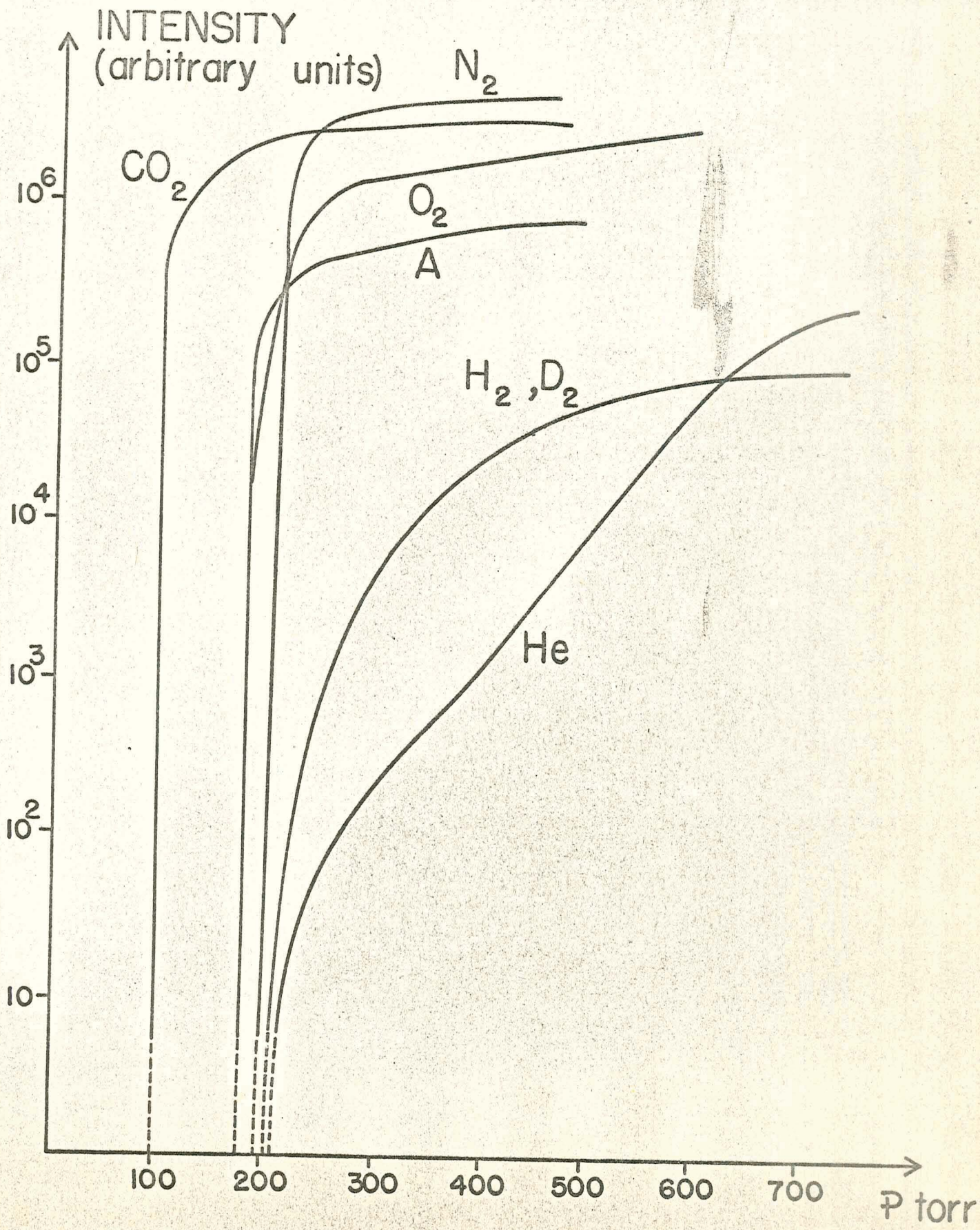

Figure 3: Bremsstrahlung light versus gas pressure

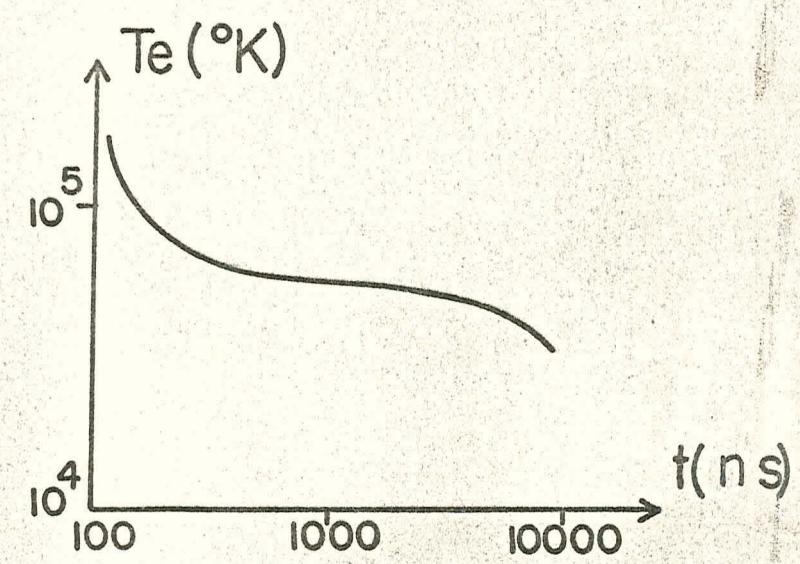

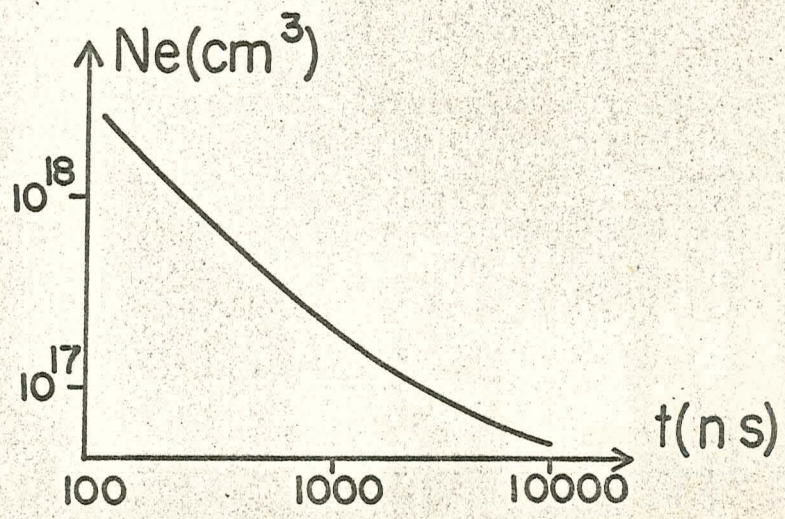

Figure 4: H_α line: electronic temperature and density at different times.

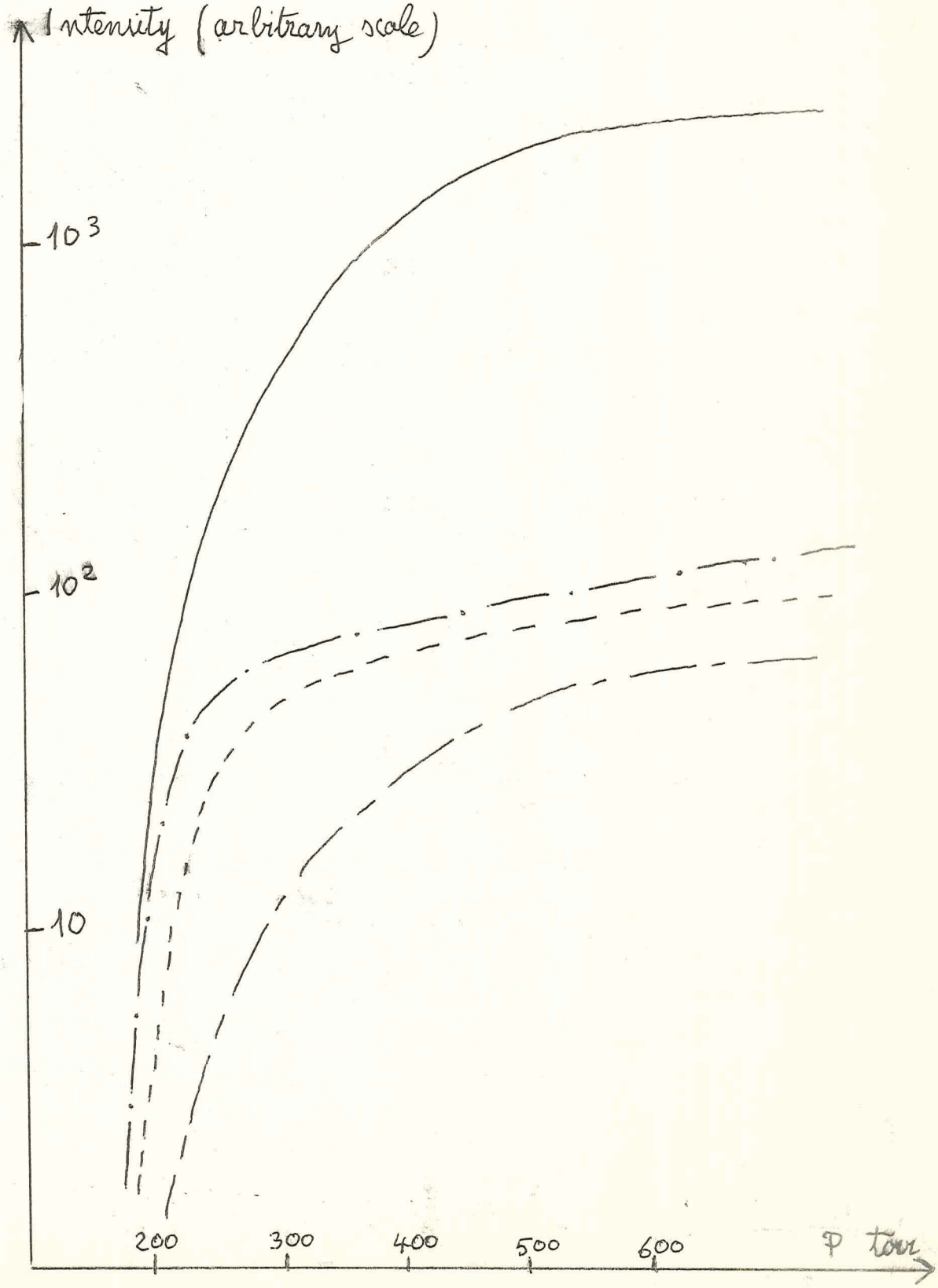

Figure 5: —— NII 4627A , —— · —— Bremsstrahlung N_2 ,

– – – H_α line , — — — Bremsstrahlung H_2 .

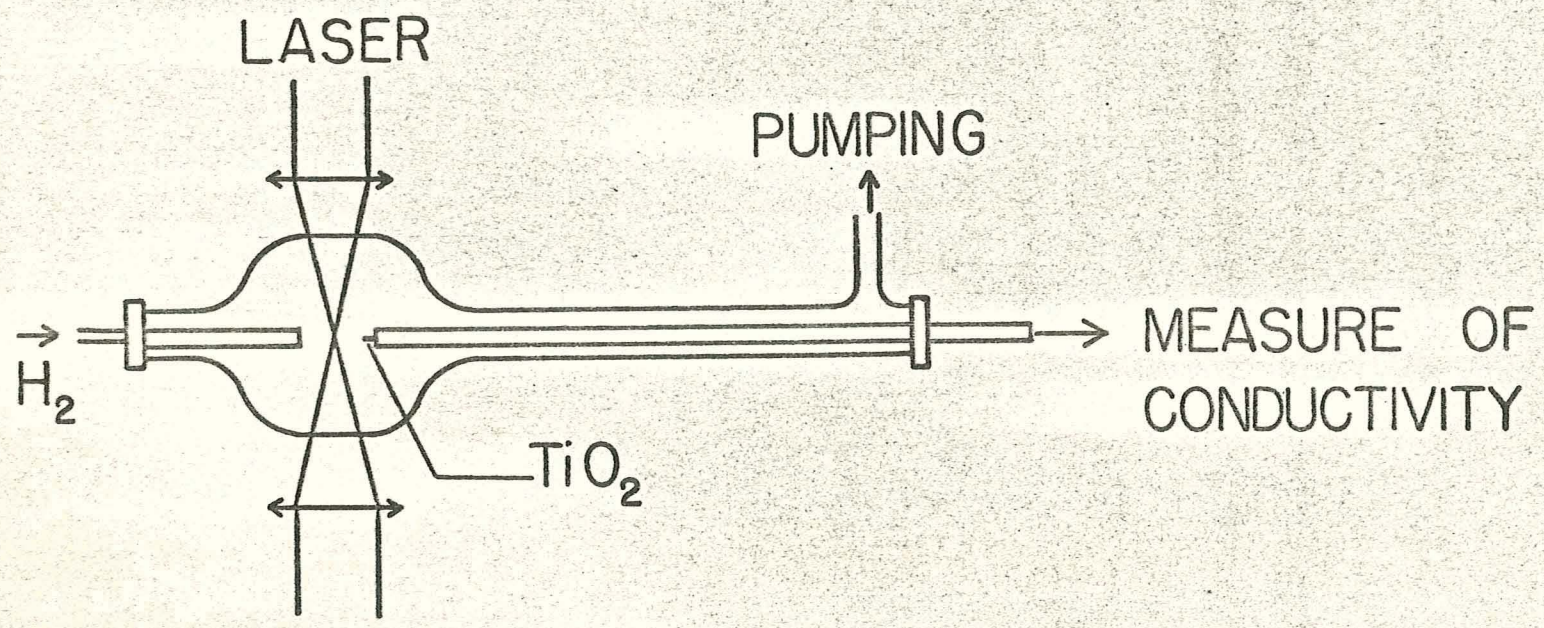

Figure 6: Direct detection of H atoms

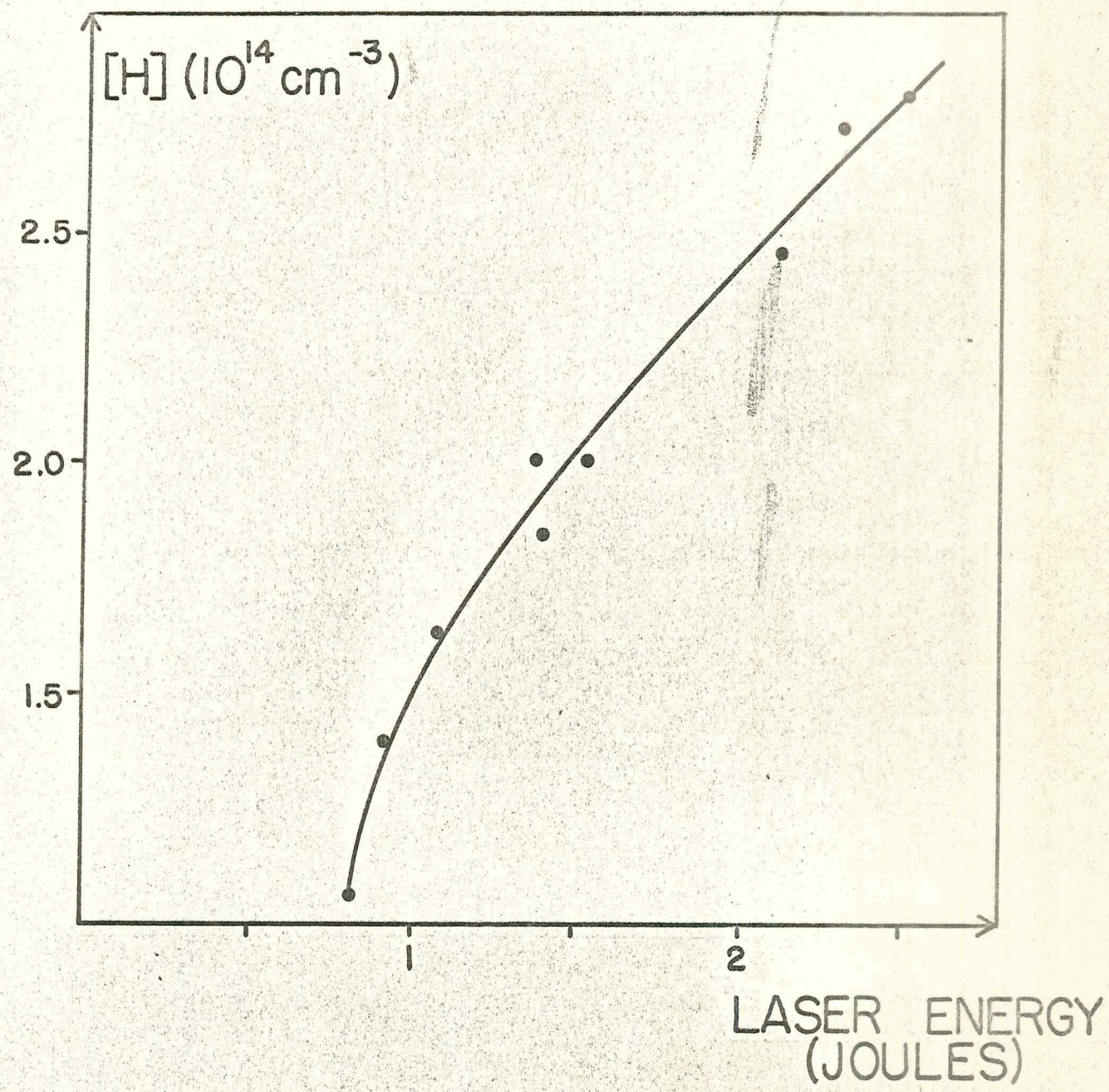

Figure 7: H concentrations in the focal volume just after the plasma extinction.

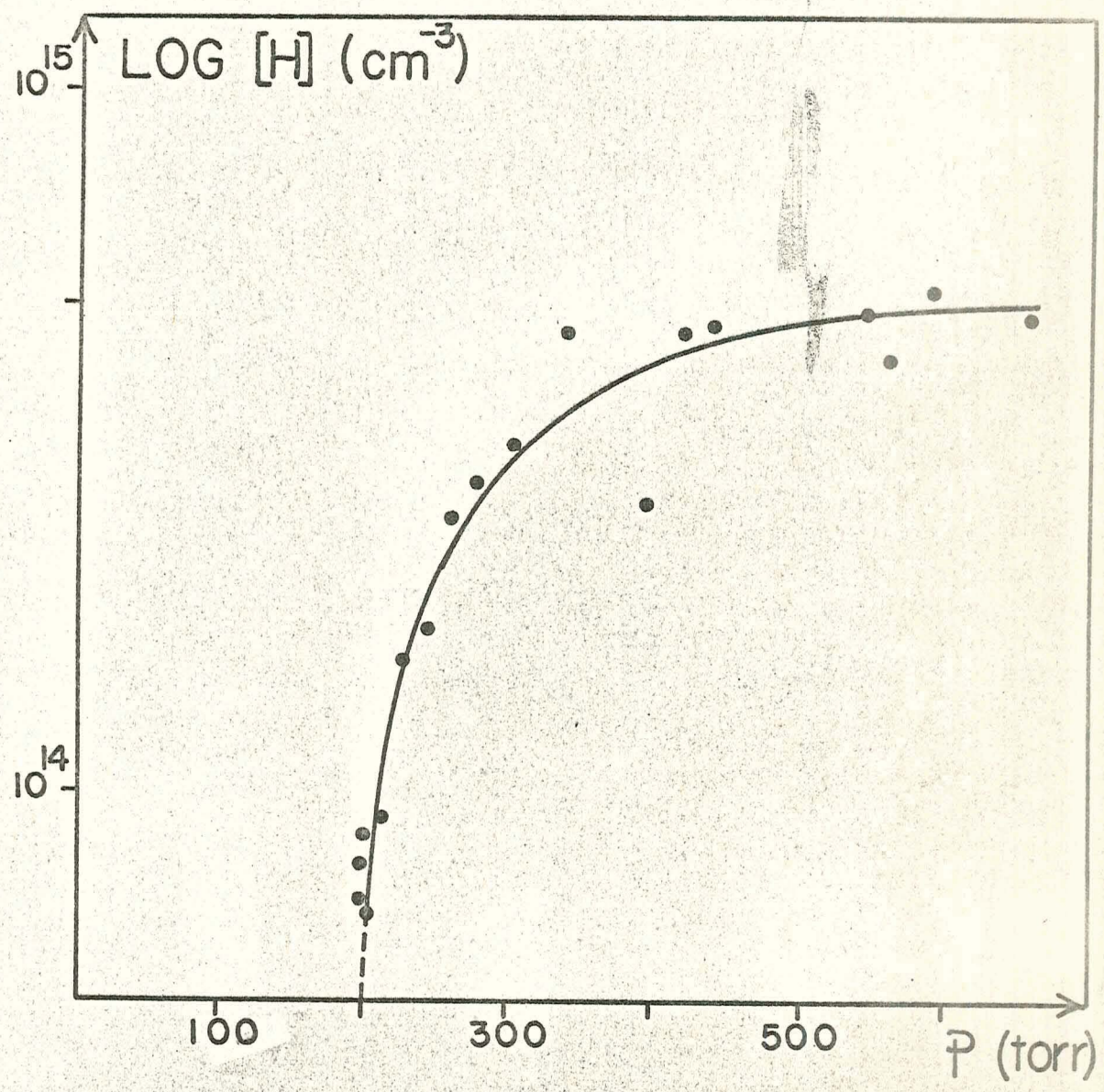

Figure 8: [H] concentrations at different pressures.

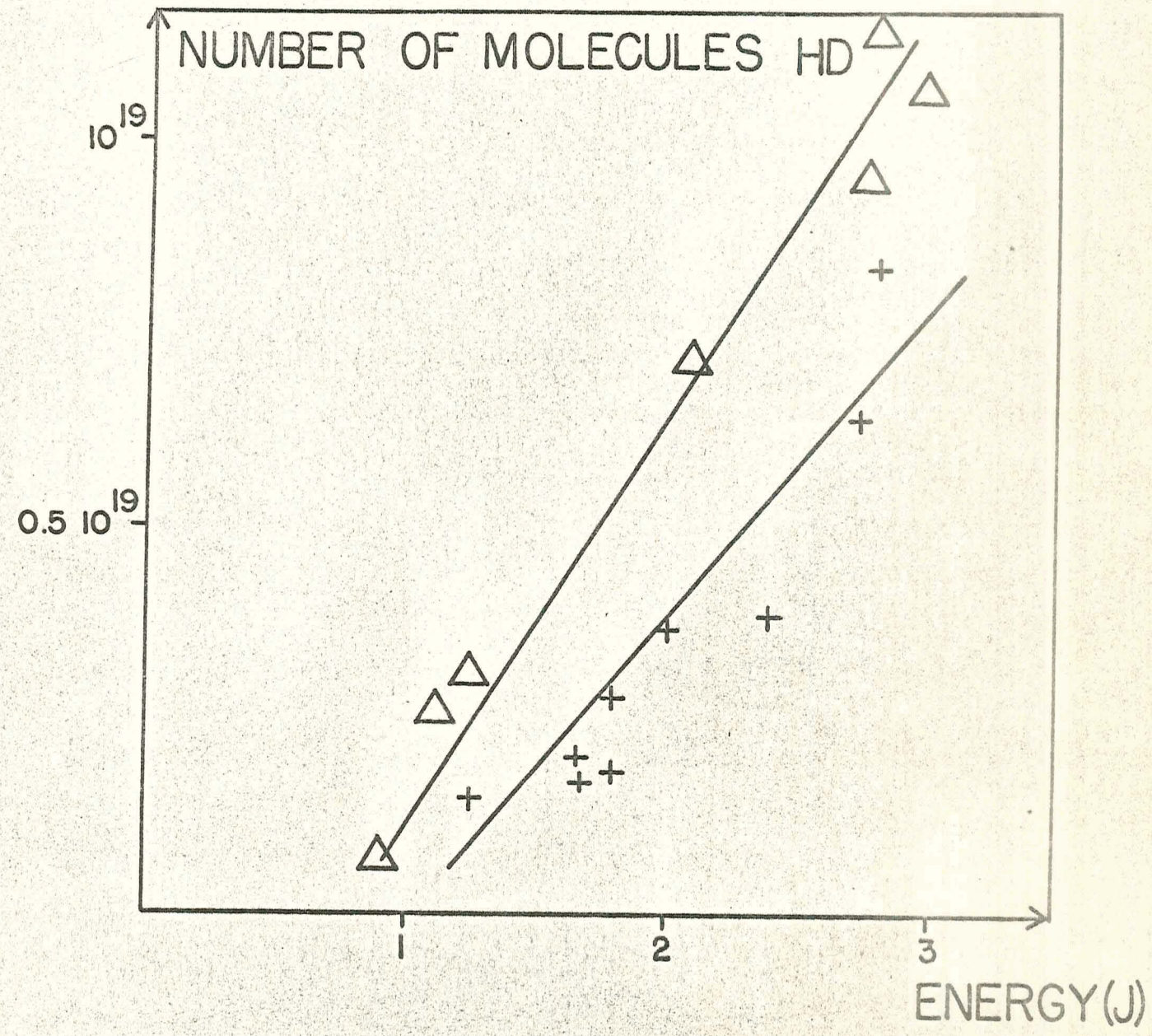

Figure 9: HD = f(E) Δ cell volume = 15 cc, † cell volume = 5 cc.

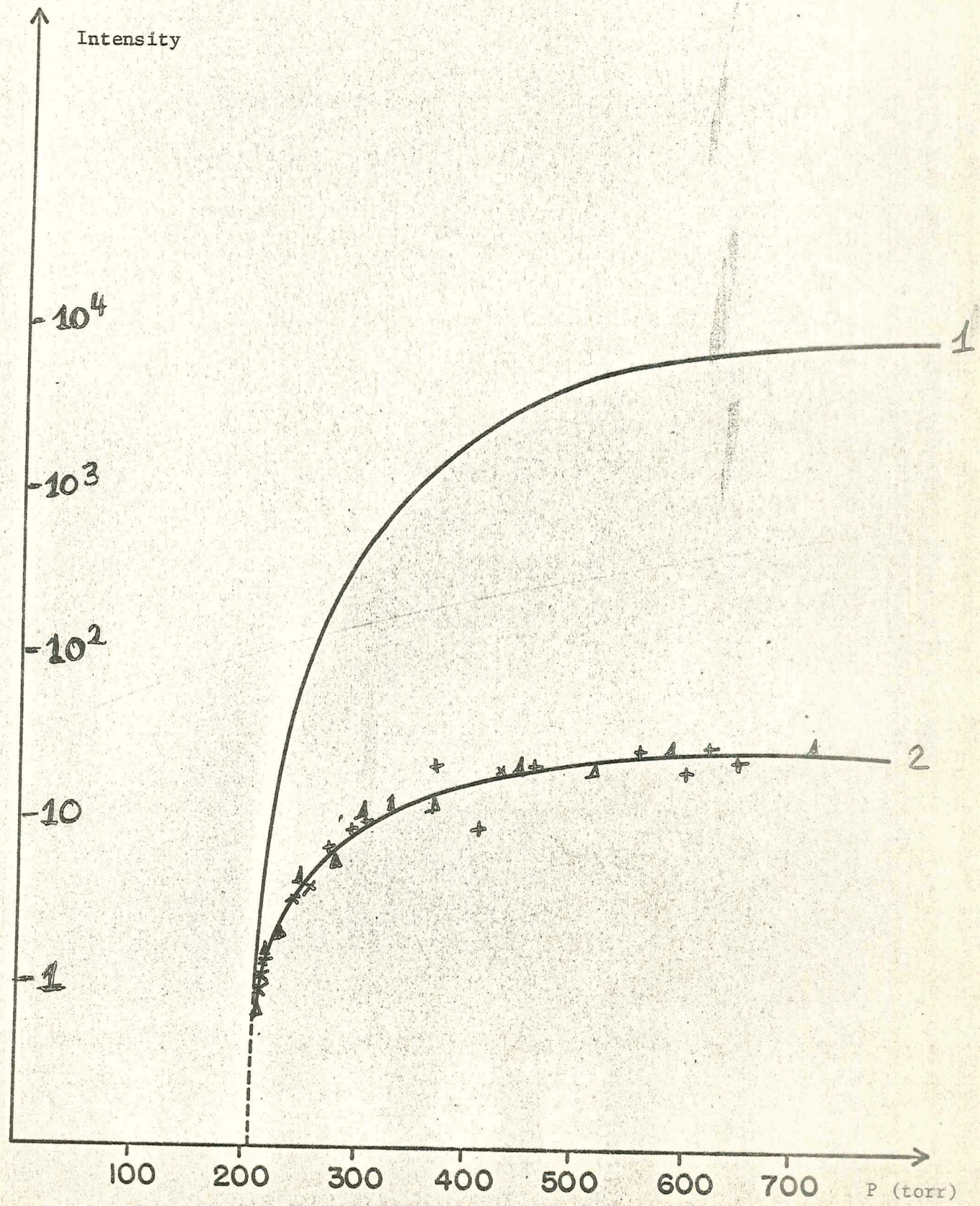

Figure 10: 1 = I. Bremsstrahlung, 2 = square root of the I. Bremsstrahlung intensity, x = [H], Δ = H_α line intensity.

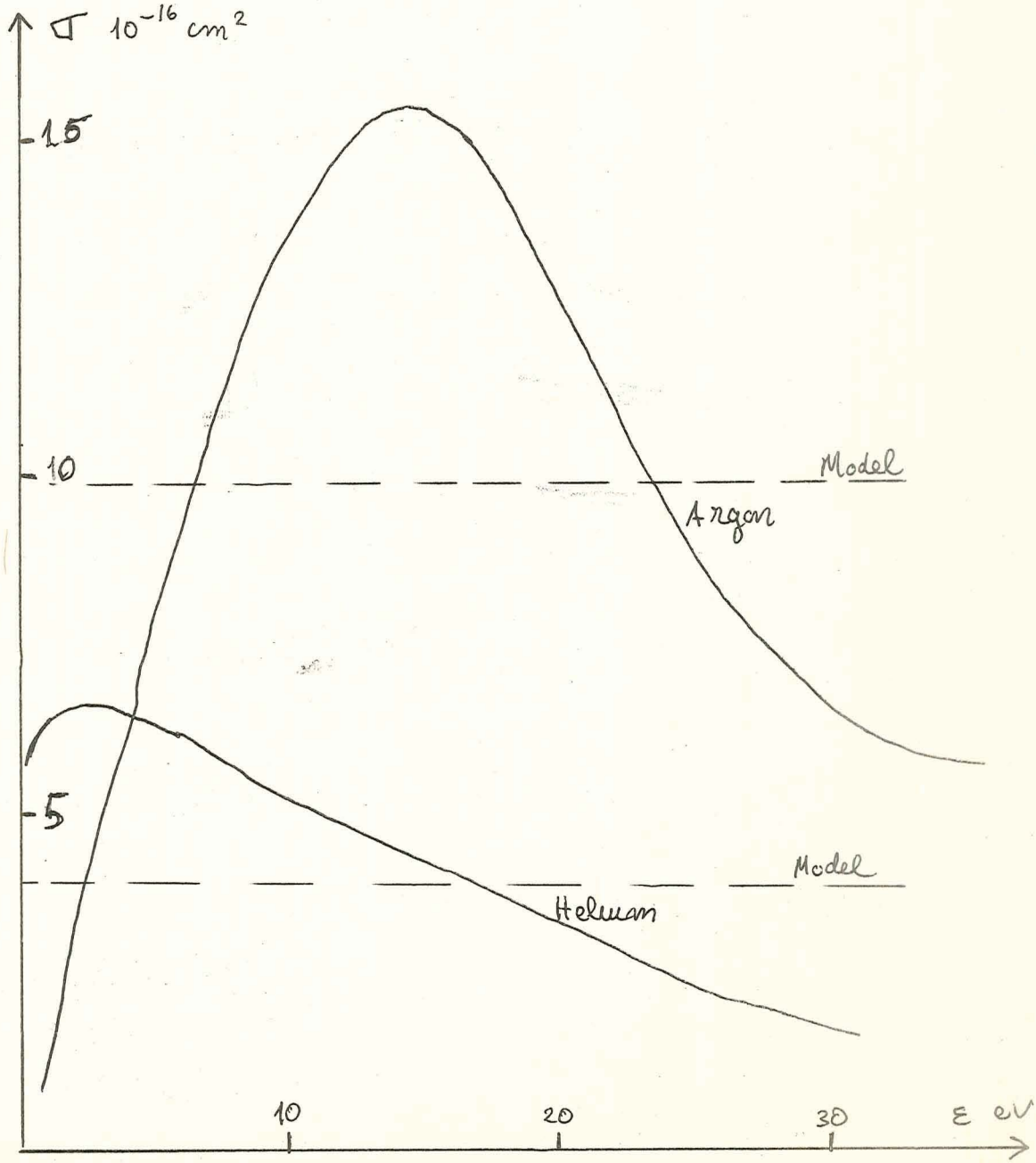

Figure 1: $\sigma(\varepsilon)$ and values used on the model calculations.

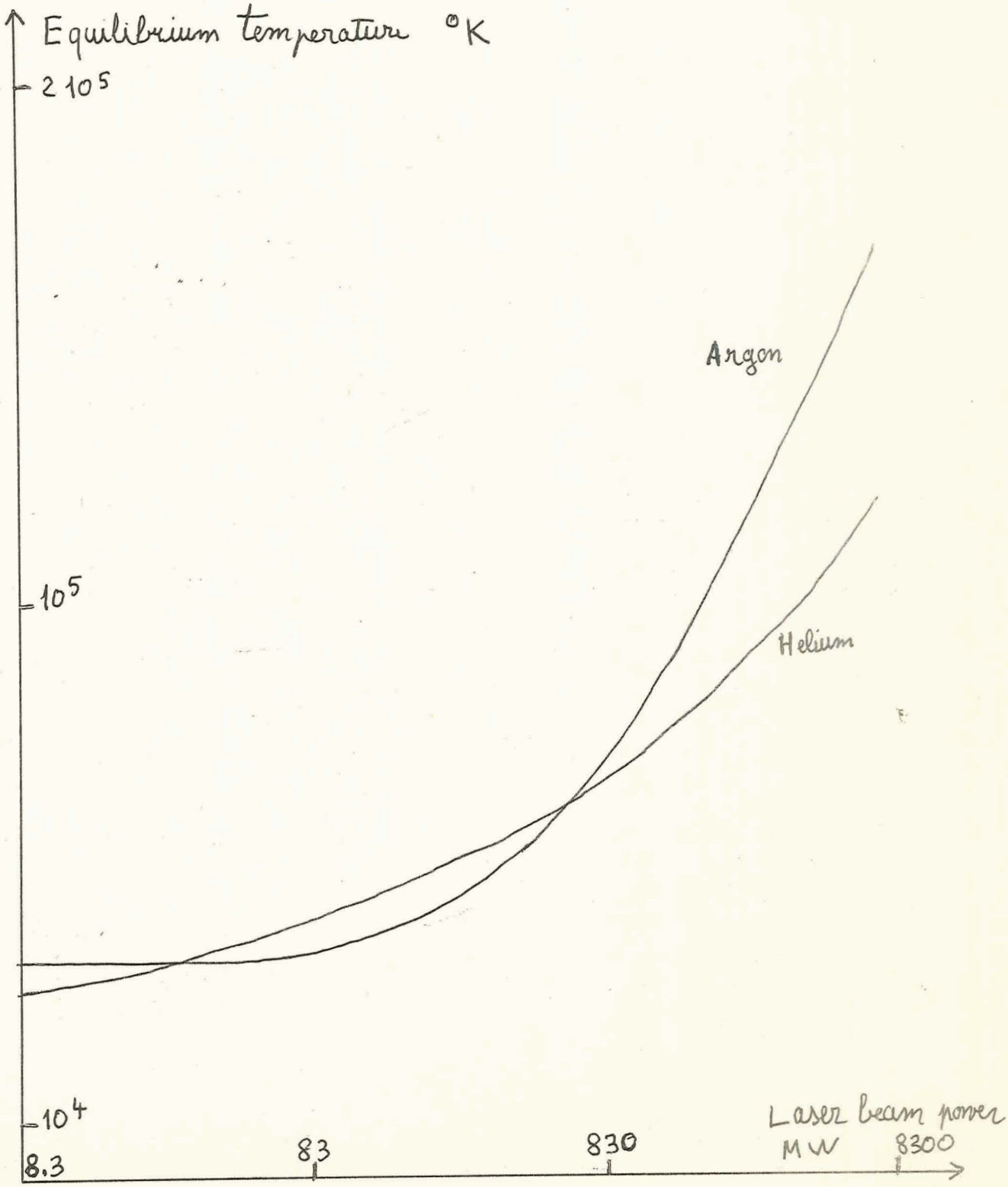

Figure 12: Equilibrium temperature for model of argon and helium as a function of the laser beam power.

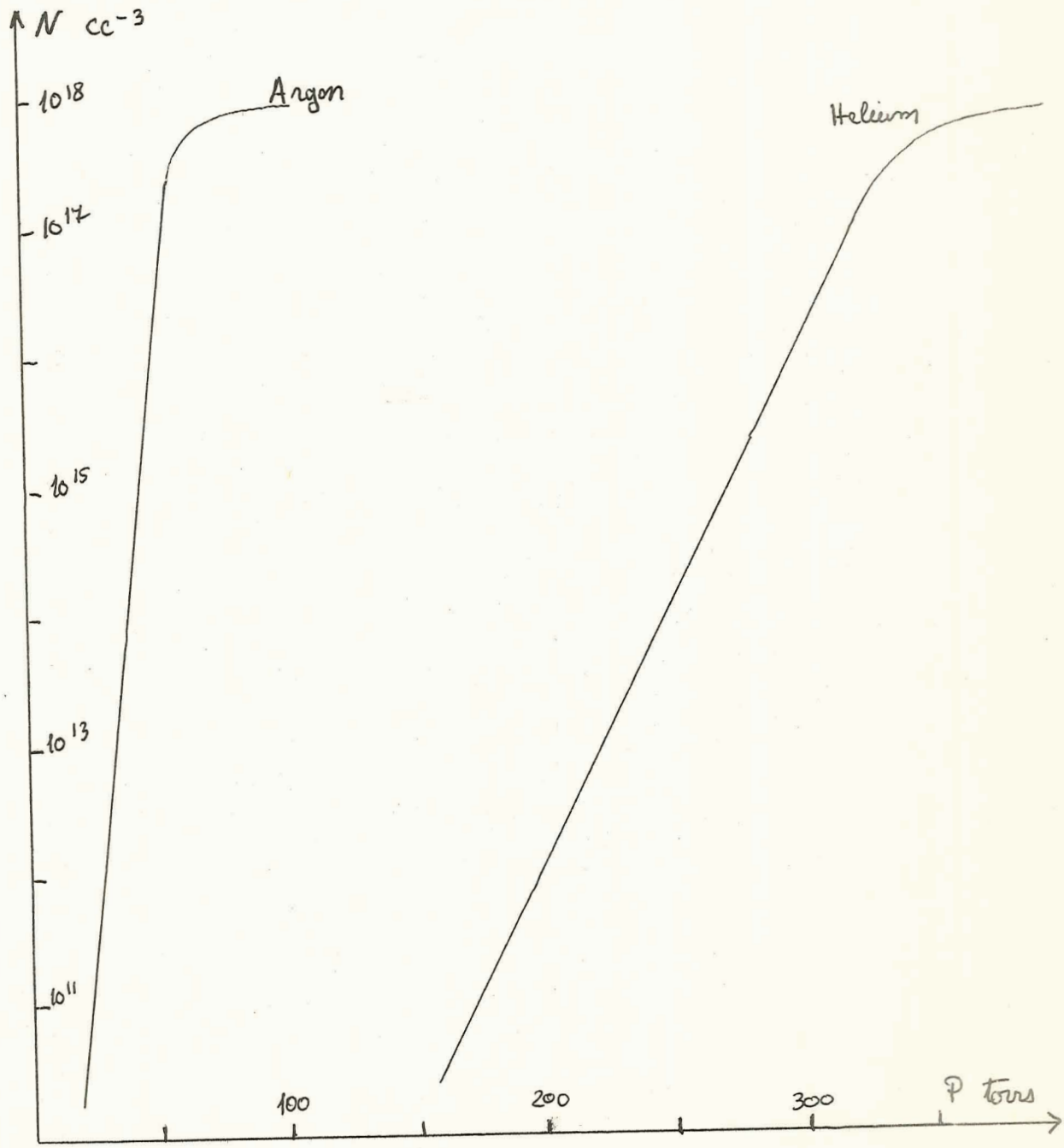

Figure 13: N(P) for helium and argon models.

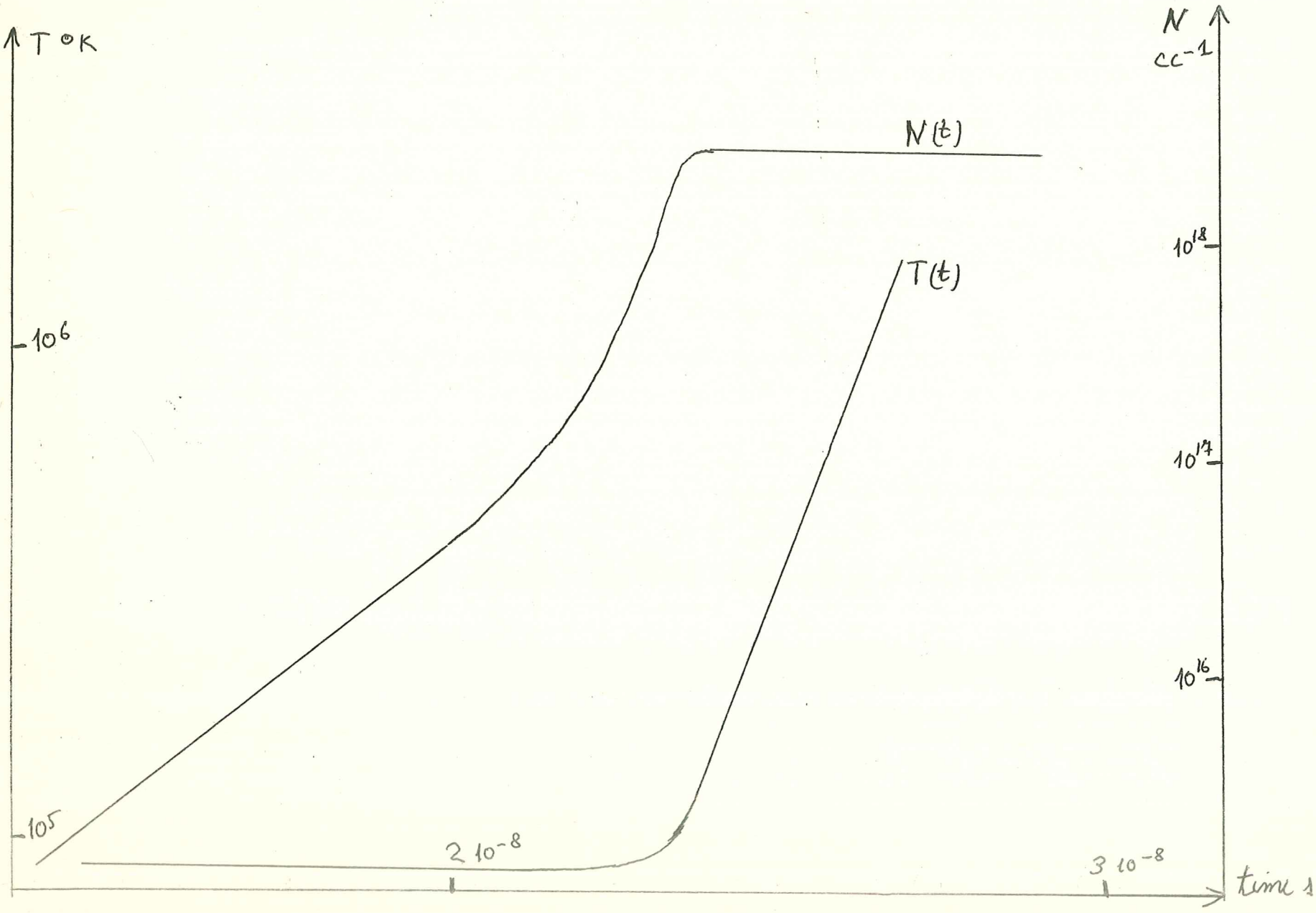

Figure 14a: Argon P = 70 torrs, influence of the inverse Bremsstrahlung electron-ion process on the electron density and temperature at different times.

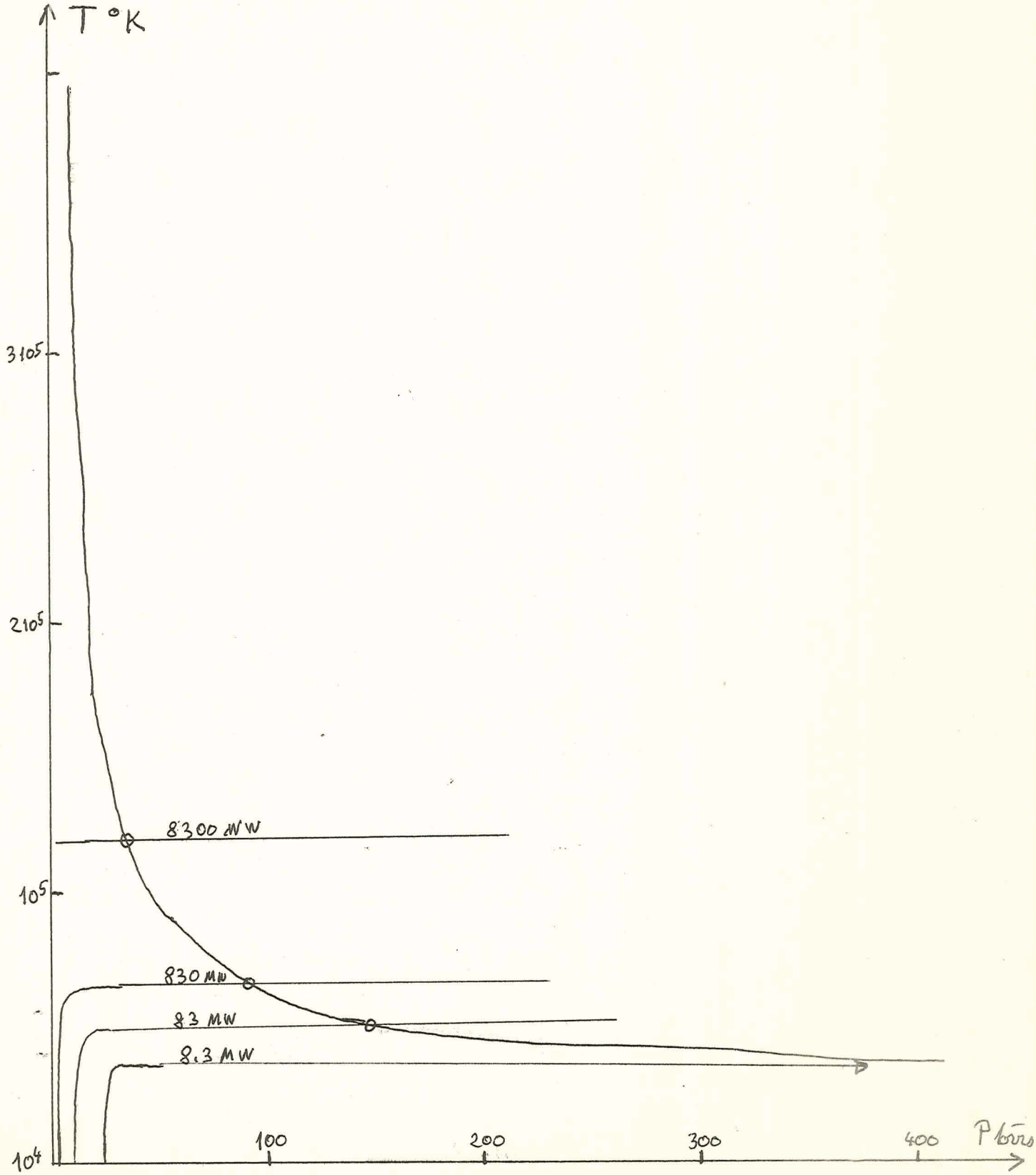

Figure 14b: Model for helium: curves T(P) determining the critical pressures.

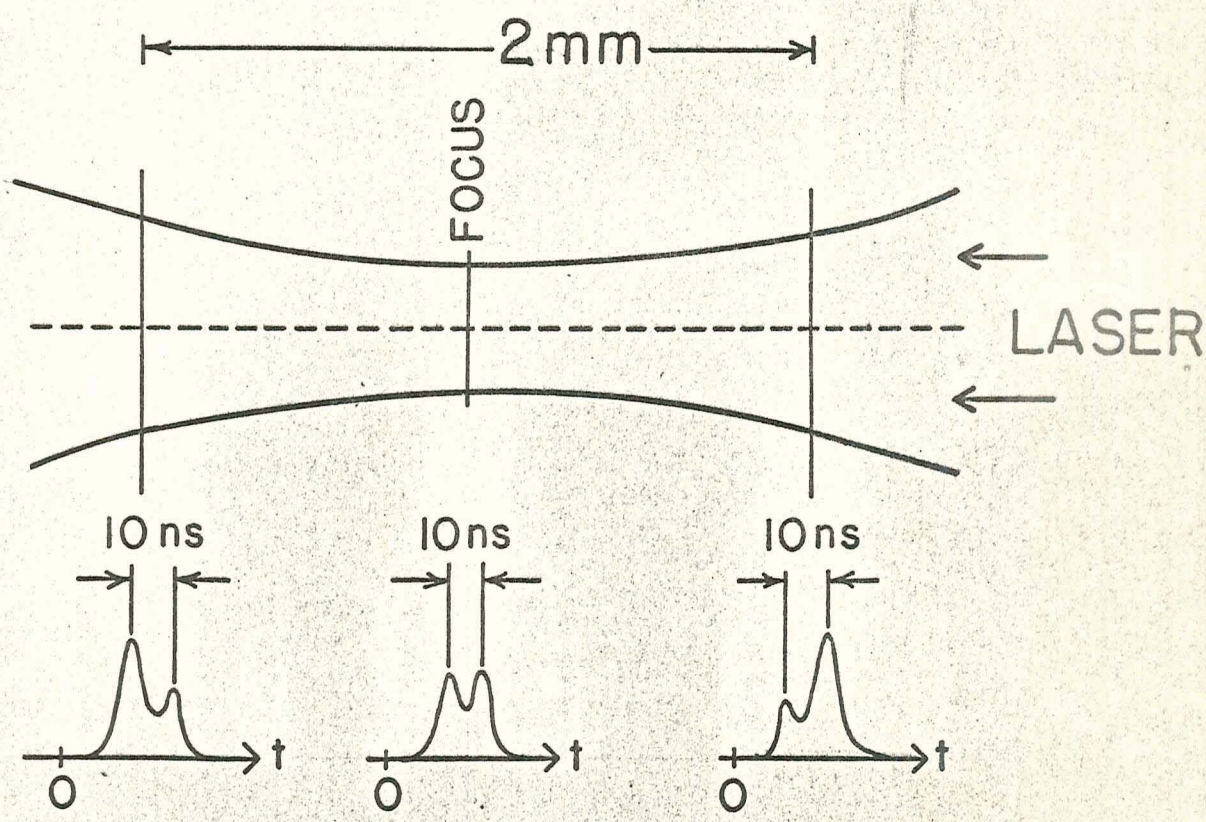

Figure 15: Light diffused out of the plasma.

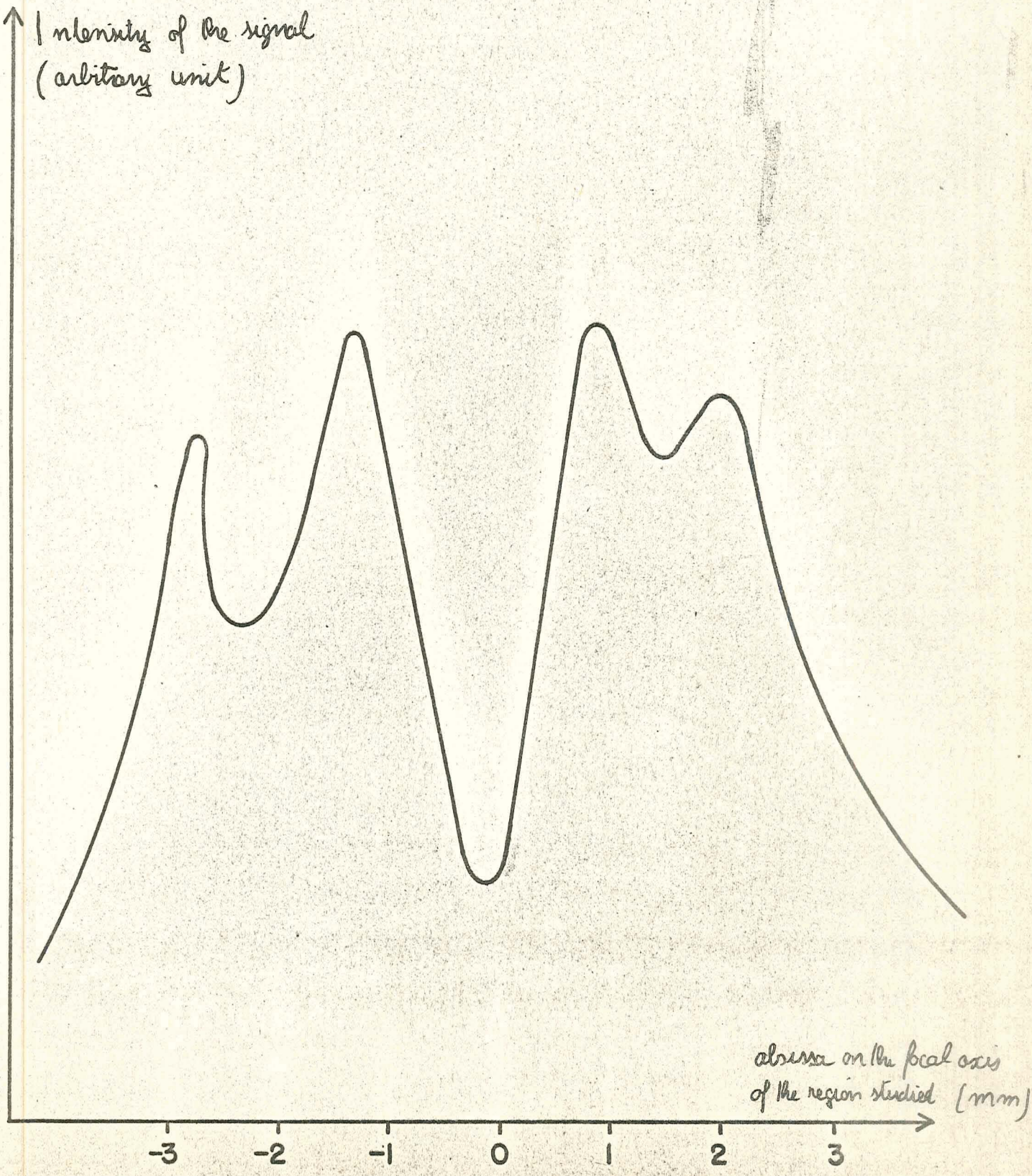

Figure 16: Brilliance of the plasma at different points.

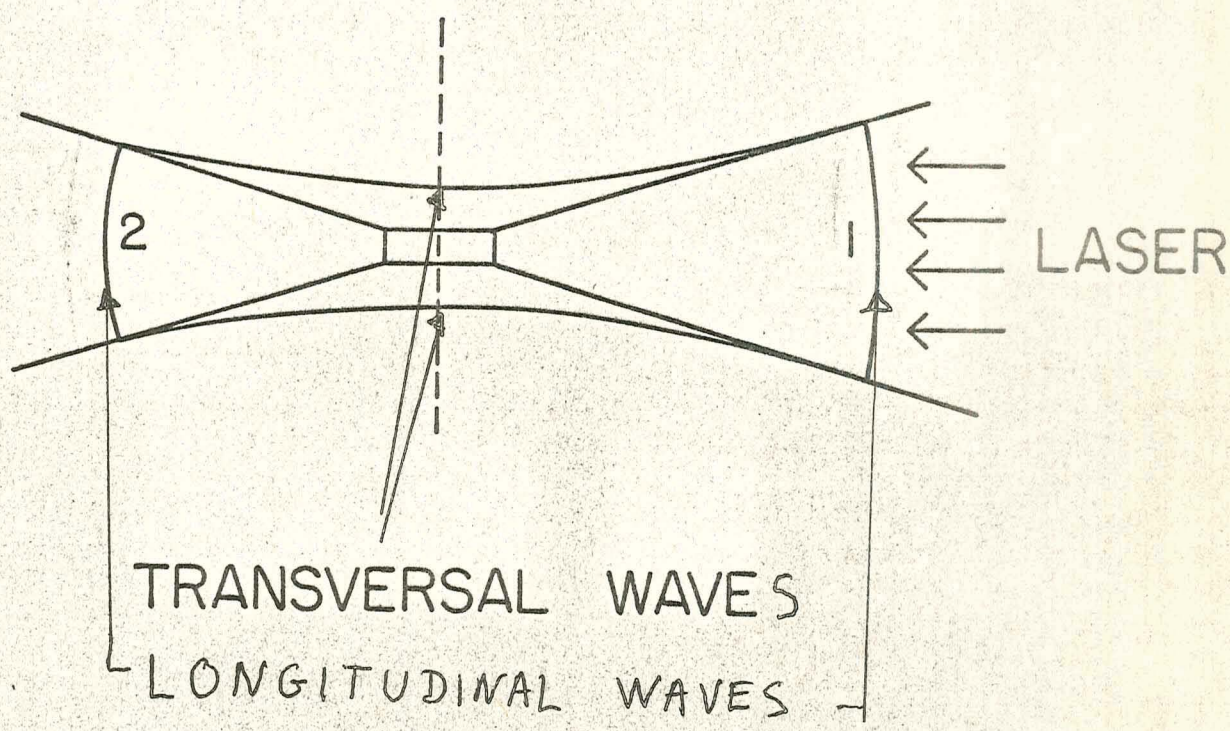

Figure 17: Geometry of the plasma.